Mesoscale Numerical Investigations of Air Traffic Emissions Over The North Atlantic During SONEX Flight 8: A Case Study

George Bieberbach, Jr.[1]
Henry E. Fuelberg[1]
Anne M. Thompson[2]
Alf Schmitt[3]
John R. Hannan[1]
G.L. Gregory[4]
Yutaka Kondo[5]
Richard D. Knabb[1]
G.W. Sachse[4]
R.W. Talbot[6]

[1]Department of Meteorology
Florida State University
Tallahassee, FL

[2]NASA Goddard Space Flight Center
Greenbelt, MD

[3]Institut für Physik der Atmosphäre
Deutsche Forschungsanstalt für Luft- und Raumfahrt
Oberpfaffenhofen, Germany

[4]NASA Langley Research Center
Hampton, VA

[5]Solar-Terrestrial Environment Laboratory
Nagoya University
Toyokawa, Aichi Japan

[6]Institute for the Study of Earth, Oceans, and Space
University of New Hampshire
Durham, NH

Corresponding author:
Henry E. Fuelberg
Department of Meteorology
Florida State University
Tallahassee, FL 32306-4520
fuelberg@met.fsu.edu

Abstract

Chemical data from flight 8 of NASA's Subsonic Assessment (SASS) Ozone and Nitrogen Oxide Experiment (SONEX) exhibited signatures consistent with aircraft emissions, stratospheric air, and surface-based pollution. These signatures are examined in detail, focussing on the broad aircraft emission signatures that are several hundred kilometers in length. A mesoscale meteorological model provides high resolution wind data that are used to calculate backward trajectories arriving at locations along the flight track. These trajectories are compared to aircraft locations in the North Atlantic Flight Corridor over a 27-33 hour period.

Time series of flight level NO and the number of trajectory/aircraft encounters within the NAFC show excellent agreement. Trajectories arriving within the stratospheric and surface-based pollution regions are found to experience very few aircraft encounters. Conversely, there are many trajectory/aircraft encounters within the two chemical signatures corresponding to aircraft emissions. Even many detailed fluctuations of NO within the two aircraft signature regions correspond to similar fluctuations in aircraft encountered during the previous 27-33 hours.

Results indicate that high resolution meteorological modeling, when coupled with detailed aircraft location data, is useful for understanding chemical signatures from aircraft emissions at scales of several hundred kilometers.

POPULAR SUMMARY

This paper investigates chemical signatures, attributed to air traffic emissions, observed during flight 8 of NASA's Subsonic Assessment (SASS) Ozone and Nitrogen Oxide Experiment (SONEX). In particular, an attempt is made to verify that these signatures were in fact due to aircraft exhaust using a high resolution meteorological model coupled with a trajectory model and simple aircraft flagging scheme. Results indicate that air traffic emissions were indeed sampled during the flight and that the chemical signatures observed were due to the superposition of 14 to 25 aircraft plumes released within the previous 27-33 hour period.

1. Introduction

Nitrogen oxides (NO_x = NO + NO_2) play a major role in the formation of tropospheric ozone (O_3). Because O_3 is a greenhouse gas, future perturbations of its global concentration could have a significant impact on climate [e.g., *Ehhalt et al.*, 1992]. Nitrogen oxides originate from a variety of natural and anthropogenic sources, including surface based fossil fuel combustion, biomass burning, lightning discharges, biogenic emissions, chemical production within the stratosphere, and aircraft emissions [*Kasibhatla*, 1993]. Previous studies have suggested that aircraft emissions are a major contributor (40%) of upper tropospheric NO_x (8 to 12 km) [*Beck et al.*, 1992]. These emissions also contain soot and various sulfur compounds that can influence both the radiative properties and formation of clouds [*Schumann et al.*, 1996]. Other recent investigations of the large scale, long term effects of jet aircraft include *Johnson et al.* [1992], *Douglass et al.* [1993], and *Brasseur et al.* [1996].

Exhaust plumes from individual jet aircraft have been examined in studies such as *Arnold et al.* [1992], *Fahey et al.* [1995], *Schulte and Schalger* [1996], *Schumann et al.* [1996], and *Whitefield et al.* [1996]. On a somewhat larger scale, *Schlager et al.* [1997] analyzed signatures of aircraft emissions in the North Atlantic Flight Corridor. They found that peak concentrations in the exhaust plumes exceeded background levels by factors of 30 (NO_x), 5 (SO_2), and 3 (CN). The emissions were attributed to aircraft that had passed their measurement leg within 5 hours prior to the observations.

The National Aeronautics and Space Administration (NASA) initiated the Subsonic Assessment (SASS) program to determine the impact of the subsonic commercial fleet on the environment. As part of this ongoing effort, the SASS Ozone and Nitrogen Oxide Experiment (SONEX) was conducted during October and November 1997. SONEX

utilized the NASA DC-8 instrumented aircraft to investigate the sources and chemistry of upper tropospheric/lower stratospheric NO_x in and near the North Atlantic Flight Corridor (NAFC). The three deployment sites for the various flights were Shannon, Ireland (52°N, 10°W); Bangor, Maine (45°N, 68°W); and the Azores (38°N, 25°W). Two test flights and fourteen science flights were performed from these locations. A more detailed discussion of the SONEX campaign is provided by *Singh et al.* [1999].

This study investigates SONEX Flight 8 in detail. A variety of chemical signatures was observed, some attributed to aircraft emissions. Our goal is to examine the origins of the aircraft emission signatures that were encountered along the DC-8 flight track, identifying the timing and locations of the aircraft that were responsible for them. To achieve these goals, we use a high resolution meteorological data set from the National Center for Atmospheric Research(NCAR)/Pennsylvania State University three-dimensional mesoscale model (MM5) [*Dudhia*, 1993; *Grell et al.*, 1994]. These data are used to calculate backward trajectories arriving at locations along the DC-8 flight track. Parcel positions then are compared to aircraft locations. The scale of our investigation differs from that of previous studies. Specifically, we examine aircraft-induced chemical signatures that were observed along several hundred kilometer segments of the DC-8 flight track, considering aircraft emissions over the entire NAFC during the previous 27-33 hour period.

2. SONEX Flight 8

2.1 The Flight

Flight 8 departed Shannon, Ireland on October 25, 1997. During this mission of ~7.5 hours duration (0815 – 1547 UTC), the DC-8 flew northeast along the western coast of Norway before turning southwest at ~ 69°N, 13°E and returning to Shannon (Figure 1). Chemical and meteorological measurements were obtained at flight levels ranging from 15,000 ft (~ 4.6 km) to 37,000 ft (~ 11.3 km). Two segments of the flight track exhibited chemical signatures consistent with aircraft emissions. These two signatures, as well as the other signatures that were encountered, are described below.

2.2 Chemical Signatures

The chemical data used in this study were extracted from a merged data set prepared by Harvard University. This set contains 10-s averages of chemical and meteorological measurements as well as flight position data for each SONEX flight. *Singh et al.* [1999] provide additional information about the various chemical measurements during SONEX.

Correlations between CO and NO indicate three distinct chemical signatures during the flight (Figure 2)--stratospheric air, air influenced by aircraft emissions, and air influenced by surface-based pollution. Stratospheric air is characterized by relatively small values of both CO and NO, while the aircraft influence is characterized by moderate CO and a range of enhanced NO. Finally, surface-based pollution is indicated in parcels having small NO but enhanced CO. These signatures, denoted STRAT, AC,

5

and POL, are indicated on the time series of flight level chemical data (Figure 3) and in the latitude-altitude diagram of flight position (Plate 1).

Two signatures suggest an aircraft influence (AC1 and AC2, Figure 3, Plate 1). The first region (AC1), sampled from ~ 31,000 - 35,500 seconds (0836 - 0952 UTC) at altitudes of 9.6 and 11.3 km, between ~ 55° N and 62° N, exhibits the weaker of the two signatures. It is characterized by enhanced values of NO_y (200 - 600 pptv), NO (30 - 400 pptv), and unheated fine aerosols (>2000 cm^{-3}). The relatively large values of the NO/NO_y ratio (0.1 - 0.7) suggest that these emissions are relatively fresh. This chemical signature is consistent with those attributed to aircraft in the NAFC by *Schalger et al.* [1997]. The CO-NO correlation during this portion of the flight (Figure 4a) also indicates the presence of aircraft emissions, as well as a small stratospheric contribution. Mixing ratios of O_3 and CO are moderate during the sampling period (30-60 ppbv and ~ 75 ppbv, respectively), indicating a relatively unpolluted background. The large spike of O_3 (~ 270 ppbv) near 35000 seconds that corresponds to a sharp decrease in CO (~ 20 ppbv) is most likely due to a brief stratospheric contribution. These observations suggest that the AC1 region contains aircraft emissions superimposed on an unpolluted background having a relatively small stratospheric contribution.

The second major chemical signature denotes air having a stratospheric origin. The STRAT region was sampled from ~35,500 - 44,000 seconds (0952 - 1213 UTC), at altitudes of 11.3, 10, and 7.5 km, between ~ 62° N and 69°N (Figure 3, Plate 1). All of the chemical tracers indicate penetration into the stratosphere. For example, large values of NO_y (500 - 1400 pptv) and O_3 (>100 ppbv) coincide with relatively small concentrations of NO (~ 20 pptv) and CO (30 - 40 ppbv). Stratospheric penetration also is apparent in the CO- NO correlation (Figure 4b) and in analyses of meteorological parameters. For

6

example, the time series of flight level potential vorticity (PV) along the DC-8's track (Figure 5) indicates a sudden increase to stratospheric values that is associated with a lowered tropopause. We assume that a potential vorticity (PV) threshold of 3.0 PV units designates the tropopause (where 1 PVU = 1×10^{-5} K mb^{-1} s^{-1}), while values > 3.0 PVU denote the stratosphere [e.g., *Fuelberg et al.*, this issue]. There is no apparent aircraft contribution in this region.

The third sampling regime (POL) consists of moderately to heavily polluted air. This region is sampled from ~ 44,000 - 52,000 seconds (1213 - 1427 UTC), at altitudes of 7.5 and 4.6 km, between ~ 69°N and 59°N (Figure 3, Plate 1). Moderate to large mixing ratios of NO_y (200-800 pptv) and CO (80-140 ppbv) correspond to near zero values of NO and NO/NO_y. Small values of unheated fine aerosol (~ 500 cm^{-3}) combined with the CO-NO signature (Figure 4c) seem to rule out an aircraft contribution.

The fourth chemical regime (AC2) lasts from ~52,000 - 56,000 seconds (1427 - 1533 UTC) between ~ 59°N and 53°N, at an altitude of 10.5 km (Figure 3, Plate 1). AC2 contains a significant aircraft signal. Broad enhancements and spikes of NO_y (200-1400 pptv), NO (50 - 500 pptv), NO/NO_y (0.2-0.8), and unheated fine aerosols (2000-9500 cm^{-3}) indicate the presence of relatively fresh aircraft emissions. The CO-NO signature in this region also indicates a relatively strong aircraft signature (Figure 4d). These enhancements again are consistent with those of *Schlager et al.* [1997].

3. Aircraft Data

We used detailed observed air traffic data from the United States Federal Aviation Administration (FAA) to investigate the aircraft influences that are indicated in the observed chemical signatures. The data set included flights over the United States, North

7

Atlantic Ocean, and Europe. The data, available at 3 minute intervals, included aircraft identification (airline + flight number), type, origin, destination, latitude, longitude, altitude, and ground speed. We examined the period October 24-25, 1997. Figure 6 shows the North Atlantic flight tracks for October 24; patterns are similar on October 25 (not shown). Eastbound traffic occurs mostly between 0100 - 0800 UTC (Figure 6a), while most westbound flights occur between 1130 - 1800 UTC (Figure 6b). Although most North Atlantic traffic occurs between these two time bounds, there is less frequent traffic at other times. The heavily traveled region between 40 - 60°N and 0 - 70°W defines the NAFC. Table 1 summarizes the number of aircraft passing through these corridors during our period of interest. Most flights occur over a small range of altitudes (Figure 7). Specifically, most eastbound aircraft (~ 200/day) flew at an altitude of 10 km, while a majority of the westbound traffic (~ 160/day) cruised at ~9.5 km.

4. Model Descriptions

4.1 Mesoscale numerical model

A high resolution meteorological data set was required to link the individual aircraft positions with the observed chemical data using backward trajectories. *Doty and Perkey* [1993] showed that hourly wind data were needed to produce reliable trajectories. This requirement was a major factor leading to our use of modeled data instead of a more coarse data source such as the European Center for Medium-range Weather Forecasting (ECMWF) 1° global analyses with its 6 hourly resolution. Other studies that have used high-resolution meteorological models to investigate chemical transport include *Wang et al.* [1996], *Pickering et al.* [1996], and *Chatfield et al.* [1996].

8

We used the non-hydrostatic version of the MM5 three-dimensional mesoscale model [*Dudhia*, 1993; *Grell et al.*, 1994] to create high resolution meteorological data. The model grid has a type-B staggering of horizontal velocity variables with respect to the thermodynamic variables [*Arakawa and Lamb*, 1977] and a sigma (terrain following) coordinate in the vertical. We employed 31 sigma levels, with an enhanced vertical resolution of ~ 20 hPa in the layer of maximum air traffic. The domain (Figure 8) consisted of a 30 km two-way interactive nest (157 x 181 grid points) centered over the NAFC, and a 90 km coarse mesh (120 x 180 points) covering a large portion of the northern hemisphere. Boundaries of the coarse domain are sufficiently distant from the inner nest to reduce the propagation of lateral boundary errors into the 30 km domain [*Warner et al.*, 1997]. The Blackadar high-resolution boundary layer scheme [*Zhang and Anthes*, 1982] and the mixed-phase explicit moisture scheme [*Reisner et al.*, 1993] were employed in both domains. The Anthes-Kuo [*Anthes*, 1977] and Kain-Fritsch [*Kain and Fritsch*, 1993] cumulus parameterizations were used for the 90 and 30 km domains, respectively. Table 2 summarizes the specifications of our simulations.

The model coarse grid was initialized at 0000 UTC October 24 using the ECMWF 2.5° global analyses provided by NCAR [*Bengtsson*, 1985; *Hollingsworth et al.*, 1986]. Sea surface temperatures were provided by the National Center for Environmental Prediction (NCEP) 2.5° global analysis. Continuous four dimensional data assimilation (FDDA) was performed on both domains during the entire forecast period (40 hours ending at 1600 UTC October 25). This assimilation is achieved by relaxing the model state toward the observed (ECMWF) state by adding artificial tendency terms to the prognostic equations that are based on the difference between the two states [*Stauffer and Seaman*, 1994]. Previous studies have found that FDDA successfully limits the

9

4.3 Aircraft Flagging Scheme

A simple flagging scheme was used to determine whether a backward trajectory encountered aircraft. The search for possible aircraft/trajectory encounters was performed at intervals of 1 hour. Due to the horizontal resolution of trajectories along the flight track (~ 30 km) and vertical resolution of the MM5 model in the upper troposphere (~ 20 hPa), we employed a 3-dimensional search volume encompassing each trajectory. The horizontal search region was defined by four corner points located 15 km north and south of the trajectory's starting and ending locations for each hourly period, while the vertical search area extended 500 meters above and below the trajectory path (a total depth of 1 km or ~50 hPa). A trajectory/aircraft encounter was assumed when an aircraft track intersected the search volume.

One should note that our simple scheme does not consider plume diffusion and deformation. Instead, we assume a 1-dimensional plume geometry (i.e., a line represents the plume), whose location is defined by the hourly aircraft flight segment (i.e. the plume is not advected or deformed within the one hour search period). Even with this simple approach, the following sections will show that the flagging results are consistent with those of the observed chemical signatures.

5. Results

5.1 MM5 Simulation

It is important to establish the credibility of the MM5 simulation by comparing results with analyses from the $1.0°$, 6-hour ECMWF global data set. Although the ECMWF data cannot resolve mesoscale features at 30 km resolution, they can be used to verify general features of the MM5 simulation. Because our trajectory calculations only

used winds from the 30 km nested grid, results from that domain are presented here.

Figure 9 contains analyses of wind speed, geopotential height, and potential vorticity at 250 hPa (~10.4 km) that were derived from ECMWF data at 1200 UTC October 25, and from the 36-hour MM5 simulation valid at the same time. Figure 9a,b shows a well defined upper level trough-ridge system dominating the North Atlantic, with a closed low over the eastern coast of Newfoundland. The undulating jet stream axis is defined by the region of strong southerly winds along the southern tip of Greenland, combined with strong northwesterly flow over the southern coast of Norway. Large values of PV associated with a depressed tropopause and tropopause folding are evident across the Norwegian Sea, western North Atlantic, and Labrador Sea (Figure 9c,d). A detailed discussion of meteorological conditions during the SONEX campaign is given in *Fuelberg et al.* [this issue].

The MM5 simulation compares favorably with the ECMWF analyses. Specifically, positions of the trough, ridge, jet stream, and closed low agree closely with the ECMWF analyses, while magnitudes of the closed low (ECMWF: <9840 m, MM5: <9960 m) and jet stream (ECMWF: >50 m s^{-1}, MM5: >40 m s^{-1}) differ only slightly (Figure 9a,b). The patterns of potential vorticity also compare favorably. The strong gradient of PV along the jet axis is comparable with the ECMWF generated gradient, as are positions and magnitudes of the various PV maxima (Figure 9c,d). Because PV is a derived quantity, involving derivatives of the horizontal wind components and temperature, any differences between the MM5 fields and global analyses are amplified. The high degree of similarity between the two versions of analyses adds credibility to our model-derived data set. This similarity extends to additional parameters at other levels

(not shown). Thus, we believe that the MM5 has produced a reliable data set that can be used for trajectory calculations and subsequent comparisons with the chemical signatures.

5.2 Trajectory Patterns

Plots of horizontal and vertical locations of trajectories arriving at the four chemical signature regions (Figure 3) are shown in Figures 10 and 11. Circles in Figure 10 indicate trajectory arrival points along the DC-8 flight track, while x's denote their starting locations, and successive arrows indicate six hour increments of travel time.

Approximately half of the trajectories arriving at chemical signature region AC1 (Figure 10a) remain within the NAFC (i.e., south of ~ 60°N, Figure 6) during the entire 27 hour integration period. The timing of these trajectories suggests that parcels encounter both eastbound (0100-0800 UTC October 24-25) and westbound (1130-1800 UTC October 24) air traffic before arriving along the DC-8 flight track. Although the remaining trajectories do not remain within the corridor during the entire integration period, they do originate in the corridor at the earliest time. The trajectories experience only minimal vertical displacements during the period (Figure 11a). Instead, they remain within the 250 to 350 hPa layer (~ 10.5 – 8 km) that encompasses the primary North Atlantic flight levels of the eastbound and westbound corridors (Figure 7). These results suggest that emissions from aircraft in the NAFC on October 24-25 have been transported to the DC-8 flight track to comprise chemical signature AC1. Later sections describe this transport in greater detail.

Few trajectories arriving in the stratospheric chemical signature region STRAT pass through the NAFC (Figure 10b); instead, they remain north of 60°N during their 29

13

hour histories. The few trajectories that do traverse the corridor are centered between ~ 250 - 200 hPa (~ 10.5 - 12 km, Figure 11b). Figure 7 indicates some aircraft within this altitude range. Therefore, some emissions may have been transported to this chemical region.

Trajectories arriving in the pollution region of the flight track (POL, Figure 3) are depicted in two segments due to the long duration of the chemical signature. Those arriving north of 65°N, denoted POL-A, remain well north of the NAFC during their 31 hour histories (Figure 10c). Although some trajectories arriving farther south (in POL-B, Figure 10d) do traverse the NAFC (Figure 6), their altitudes (below ~350 hPa, 8.2 km, Figure 11d) are below those of the organized flight levels (Figure 7). Therefore, it is unlikely that significant aircraft emissions from the corridor are included in the pollution segment. Instead, five day back trajectories calculated from the ECMWF data (not shown) suggest that the pollution originates over portions of North America.

Trajectories arriving within the final chemical region, AC2 (Figure 10e), have the greatest likelihood of encountering aircraft emissions during their 33 hour histories. Every trajectory not only passes through the NAFC (Figure 6), but most remain within the corridor throughout the entire period. Altitudes of the trajectories are between ~ 250 - 500 hPa (10.4 – 5.6 km, Figure 11e), encompassing many flight levels within the corridor (Figure 7). The timing and location of these trajectories suggest that emissions from both eastbound and westbound traffic are transported to the DC-8 sampling region.

5.3 Aircraft-Trajectory Encounters

Table 4 quantifies the trajectory/aircraft encounters for each chemical signature region (Figure 3) based on the methodology described in Section 4.3. Trajectories

arriving in regions AC1 and AC2 encounter the most aircraft during their lifetimes. 77 and 146, respectively. Trajectories arriving in AC1 encounter aircraft from the eastbound corridors on October 24 and 25, the westbound corridor on October 24, and during the three intermediate periods. The AC2 region is the only segment to receive input from all four corridors and all intermediate times. On the other hand, only 16 aircraft are encountered by trajectories arriving within the stratospheric region. These encounters mostly occur prior to 1800 UTC October 24. Trajectories arriving along the first half of the pollution region (POL-A) encounter no aircraft, while trajectories comprising POL-B experience only 3 encounters before arrival.

It is informative to examine in detail the trajectory/aircraft encounters comprising chemical region AC2, i.e., which is the best defined aircraft emissions signature. Examples are shown in Plate 2, where trajectory locations are denoted by circles, and aircraft locations are denoted by asterisks. Pink symbols indicate that no trajectory/aircraft encounter occurs based on the specifications in Section 4.3, while blue symbols indicate that a trajectory/ aircraft encounter does occur. One should note that encounters are based on trajectory and aircraft paths over a 1-hour interval, while only locations at the ending hour are shown in the Plate. The first hour of the backward trajectory run (Plate 2a, 1500-1400 UTC October 25) is during the westbound corridor period. Since a majority of the westbound air traffic is located west of 30°W, there are no encounters because the trajectories still are very near the DC-8 flight track. However, as the trajectories travel westward (backward in time), they reach aircraft in the westbound corridor (Plate 2b). Nonetheless, due to the north-south orientation of the trajectory axis, few aircraft are encountered by the trajectories. One should note that aircraft positions clearly denote the organization of the east-west flight tracks that during these active

15

corridor periods (Plates 2a, 2b, 2d, 2e, 2g, 2h). However, aircraft traversing the Atlantic during the intermediate periods are less organized and in fewer numbers (Plates 2c, 2f). As the simulation continues, the axis of the backward trajectories rotates counterclockwise due to the upper level ridge located over the eastern Atlantic (Figure 9). This effectively shifts the northern segment of trajectories into the NAFC, setting the stage for numerous encounters with both eastbound and westbound air traffic (Plates 2d, 2e, 2g, 2h). The axis of the trajectories eventually becomes oriented west to east, producing a large number of trajectory/aircraft encounters. This orientation explains the significant emissions signature observed in AC2.

Figure 12 relates the aircraft encounters to the various chemical signatures in Figure 3. It contains the number of aircraft encountered by each trajectory arriving along the DC-8 flight track (trajectories arrive at 1 minute intervals), along with the time series of flight level NO. We chose NO because it is a major exhaust species and its decay is minimal over the 33 hour period of our longest trajectories. One should note that the overall structure of the two time series is strikingly similar. For example, the near zero values of NO in the polluted region (POL) correspond to the absence of aircraft encounters (except for three encounters near the start of AC2). Most of the STRAT region also exhibits very small NO and few aircraft encounters. The small number of encounters near 36000 and 41000 seconds corresponds to the regions of slightly enhanced NO, although there is a small temporal displacement between the encounters and the chemical signature at 44000 seconds.

The agreement between NO and numbers of aircraft encounters are impressive within regions AC1 and AC2 (Figure 12). In general, these signature regions exhibit many more aircraft encounters than observed in the STRAT and POL regions. Several

specific maxima and minima are denoted by numbers in the figure. Specifically, the magnitude and timing of peak 1 (14 encounters) and minimum 2 (2 encounters) compare favorably with the maximum (~ 375 pptv) and minimum values of NO (~25 pptv) occurring near 31500 and 32500 seconds, respectively. Within region AC2, three maxima (numbered 3, 4, and 6) and one minimum (denoted 5) are apparent in both the aircraft and NO plots. The timing (~ 52000 and 52500 seconds) and relative magnitudes of peaks 3 (21 encounters) and 4 (18 encounters) are consistent with the corresponding NO spikes (~ 200 and 175 pptv). The small number of encounters (3) occurring at ~ 53500 seconds (denoted 5) compares favorably in both timing and magnitude to the minimum in the NO mixing ratio (~ 50 pptv). The last maximum (numbered 6 near 55000 seconds) represents the greatest number of aircraft encounters (25 encounters) of all the four chemical regions. The NO mixing ratio also is a relative maximum (~ 450 pptv), although it is exceeded by two greater maxima (~ 500 pptv) at slightly earlier times. These two earlier spikes in NO do not correspond to maxima in aircraft encounters. They may represent very fresh emissions that have not yet undergone significant diffusion. The timing of trajectory/aircraft encounters is not considered in our scheme. Nonetheless, these results confirm that aircraft emissions are indeed responsible for the pronounced chemical signatures observed in regions AC1 and AC2. Specifically, it appears that the major signatures are due to the superposition of 14 to 25 aircraft plumes within the past 33 hours.

6. Summary and Conclusions

Flight 8 of NASA's Subsonic Assessment (SASS) Ozone and Nitrogen Oxide Experiment (SONEX) originated in Shannon, Ireland on October 25, 1997 and flew

northwest along the west coast of Norway before turning southwest at ~ 69°N, 13°E and returning to Shannon. The *in situ* chemical data indicated three types of chemical signatures—stratospheric air, two regions of aircraft emissions, and a region of surface-based pollution. We have examined these signatures in detail, focussing on the aircraft emission signatures.

We used the National Center for Atmospheric Research/Pennsylvania State University three-dimensional mesoscale model (MM5) to create a high resolution three dimensional meteorological data set. The model was configured with two way interactive nesting, i.e., with a 90 km outer grid and a finer 30 km internal grid that encompassed the flight region. Analyses from the MM5 simulation agreed closely with global analyses. Therefore, the MM5 output, available at hourly intervals, was used to calculate backward trajectories arriving along the flight track at 1-minute (~30 km) intervals. We believe that the MM5-derived data set provided a better representation of actual wind regimes and, consequently, more accurate trajectories than is possible using global data that typically are at 6 hourly intervals and horizontal grid intervals of ~110 km. The improved resolution from the MM5 is important since trajectories are very sensitive to slight errors in both wind direction and speed, as well as the temporal frequency of the wind data [e.g., Doty and Perkey, 1993]. Detailed information about aircraft locations and altitudes also was available. A simple flagging scheme was used to determine when a trajectory encountered aircraft within the North Atlantic Flight Corridor.

The DC-8 passed through a region of stratospheric air at altitudes of 11.3, 10, and 7.5 km between ~ 62° N and 69°N. The chemical signature included enhanced NO_y (500 - 1400 pptv) and O_3 (>100 ppbv) along with reduced NO (~ 20 pptv) and CO (30 - 40

18

ppbv). Values of potential vorticity at flight level exceeded the commonly accepted stratospheric threshold. Few trajectories arriving at the stratospheric chemical signature had passed through the NAFC during their 29 hour histories.

The DC-8 also sampled a region of moderately to heavily polluted air at altitudes of 7.5 and 4.6 km between ~ 69°N and 59°N. This chemical signature included moderate to large mixing ratios of NO_y (200-800 pptv) and CO (80-140 ppbv) and near zero values of NO and NO/NO_y. Small values of unheated fine aerosol (~ 500 cm^{-3}) together with the CO-NO signature seemed to rule out an aircraft contribution. And, trajectories arriving along the northern portion of the pollution signature remained well north of the NAFC during their 31 hour histories. Although some trajectories arriving farther south along the signature did originate or pass through the NAFC, their altitudes were below those of the organized flight tracks. Five day backward trajectories calculated from a global data set indicated that the pollution originated over North America.

The first chemical signature consistent with aircraft emissions was sampled on the DC-8's outbound flight leg at altitudes of 9.6 and 11.3 km between ~ 55° N and 62° N. This region was characterized by enhanced values of NO_y (200 - 600 pptv), NO (30 - 400 pptv), and unheated fine aerosols (>2000 cm^{-3}). Relatively large values of the NO/NO_y ratio (0.1 - 0.7) suggested that these emissions were relatively fresh. Mixing ratios of O_3 and CO were moderate throughout the entire sampling period (30-60 ppbv and ~ 75 ppbv, respectively), indicating a relatively unpolluted background. A brief spike of O_3 (~ 270 ppbv), corresponding to a sharp decrease in CO (~ 20 ppbv), suggested a brief stratospheric contribution.

Approximately half of the trajectories arriving at this chemical signature remained within the NAFC during the entire 27 hour computational period. The remaining

19

trajectories did not remain within the corridor during the entire period, but did originate in the corridor. The trajectories remained within the 250 to 350 hPa layer (~ 10.5 – 8 km) that encompassed the primary North Atlantic flight levels.

The second chemical signature corresponding to aircraft emissions occurred during the return flight leg between ~ 59°N and 53°N at an altitude of 10.5 km. The chemical data suggested a significant aircraft signal. Broad enhancements and spikes of NO_y (200- 1400 pptv), NO (50 - 500 pptv), NO/NO_y (0.2-0.8), and unheated fine aerosols (2000-9500 cm^{-3}) indicated relatively fresh aircraft emissions. The CO-NO signature also indicated a relatively strong aircraft signature.

Every trajectory that arrived at this chemical signature passed through the NAFC, and most remained within the corridor throughout the entire 33 hour computational period. Altitudes of these trajectories, between ~ 250 - 500 hPa (10.4 – 5.6 km), corresponded to many flight levels within the corridor.

There was excellent agreement between a time series of flight level NO and the numbers of aircraft encountered by trajectories arriving along the flight track. Near zero values of NO in the polluted region corresponded to the absence of aircraft encounters. Most of the stratospheric region also contained very small NO and very few aircraft encounters. On the other hand, the two regions with an aircraft emissions signature exhibited many more aircraft encounters than observed in the stratospheric and pollution regions. Several specific maxima and minima of NO corresponded to similar features in the numbers of aircraft encounters. The major aircraft signatures corresponded to the superposition of 14 to 25 aircraft plumes within the previous 27-33 hours.

In summary, the results indicate that high resolution meteorological modeling coupled with detailed aircraft location data is useful for understanding chemical signatures from aircraft emissions at scales of several hundred kilometers.

Acknowledgements

References

Anthes, R.A., A cumulus parameterization scheme utilizing a one-dimensional cloud model, *Mon. Wea. Rev.*, *105*, 270-286, 1977.

Arakawa, A., and V.R. Lamb, Computational design of the basic dynamical process of the UCLA general circulation model, *Methods in Computational Physics*, *17*, Academic Press, 173-265, 1977.

Arnold, F.J., J. Scheid, T. Stilp, H. Schlager, and M.E. Reinhardt, Measurements of jet aircraft emissions at cruise altitude, I: The odd-nitrogen gases NO, NO_2, HNO_2 and HNO_3, *Geophys. Res. Lett.*, 19, 2421-2424, 1992

Beck, J.P., C.E. Reeves, F.A.A.M. de Leeuw, and S.A. Penkett, The effect of aircraft emissions on tropospheric ozone in the northern hemisphere, *Atmos. Env.*, *26A*, 17-27, 1992.

Bengtsson, L., Medium-range forecasting--The experience of ECMWF, *Bull. Amer. Meteorol. Soc.*, *66*, 1133-1146, 1985.

Board, A.S., H.E. Fuelberg, G.L. Gregory, B.G. Heikes, M.G. Schultz, D.R. Blake, J.E. Dibb, S.T. Sandholm, and R.W. Talbot, Chemical characteristics of air from differing source regions during PEM-Tropics A, *J. Geophys. Res.*, in press, 1999.

Brasseur, G.P., J.F. Muller, and C. Granier, Atmospheric impact of NOx emissions by subsonic aircraft: A three dimensional model study, *J. Geophys. Res.*, 101, 1423-1428, 1996

Chatfield, R.B., J. A. Vastano, H.B. Singh, and G. Sachse, A general model of how fire emissions and chemistry produce African/oceanic plumes (O_3, CO, PAN, smoke) in TRACE A, *J. Geophys. Res.*, *101*, 24279-24306, 1996.

Doty, K.G., and D.J. Perkey, Sensitivity of trajectory calculations to temporal frequency of wind data, *Mon. Wea. Rev.*, *121*, 387-401, 1993.

Douglass, A.M., R.B. Rood, C.J. Weaver, M.C. Cerniglia, And K.F. Brueske, Implications of three-dimensional tracer studies for two-dimensional assessments of the impact of supersonic aircraft on stratospheric ozone, *J. Geophys. Res.*, 98, 8949-8963, 1993

Dudhia, J., A nonhydrostatic version of the Penn State-NCAR mesoscale model: Validation tests and simulation of an Atlantic cyclone and cold front, *Mon. Wea. Rev.*, *121*, 1493-1513, 1993.

Ehhalt, D.H., F. Rohrer, and A. Wahner, Sources and distribution of NO_x in the upper troposphere at northern mid-latitudes, *J. Geophys. Res.*, *97*, 3725-3738, 1992.

Fahey, D.W., et al., Emission measurements of the Concorde supersonic aircraft in the lower stratosphere, *Science*, 270, 70-74, 1995.

Fuelberg, H.E., R.O. Loring Jr., M.V. Watson, M.C. Sinha, K.E. Pickering, A.M. Thompson, G.W. Sachse, D.R. Blake, and M.R. Schoeberl, TRACE A trajectory intercomparison 2. Isentropic and kinematic methods, *J. Geophys. Res.*, *101*, 23927-23939, 1996.

Fuelberg, H.E., R.E. Newell, S.P. Longmore, Y. Zhu, D.J. Westberg, E.V. Browell, D.R. Blake, G.R. Gregory, and G.W. Sachse, A meteorological overview of the Pacific Exploratory Mission (PEM)-Tropics period, *J. Geophys. Res.*, in press, 1999.

Fuelberg, H.E., J.R. Hannan, P.F.J.van Velthoven, E.V. Browell, G. Bieberbach Jr., R.D.

Knabb, K.E. Pickering, H.B. Selkirk, A meteorological overview of the SONEX period, *J. Geophys. Res.*, this issue.

Garstang, M., P.D. Tyson, R. Swap, M. Edwards, P. Kallberg, and L.A. Lindesay, Horizontal and vertical transport of air over southern Africa, *J. Geophys. Res.*, *101*, 23721-23736, 1996.

Grell, G.A., J. Dudhia, and D.R. Stauffer, A description of the fifth-generation Penn State/NCAR mesoscale model (MM5), *Tech. note, NCAR/TN-398+STR.* 138pp., Natl. Cent. Atmos. Res., 1994.

Hannan, J.R., H.E. Fuelberg, A.M. Thompson, G. Bieberbach Jr., R.D. Knabb, H.B. Selkirk, K.E. Pickering, Y. Kondo, and D.D. Davis, Atmospheric chemical transport based on high resolution model-derived winds: A case study, *J. Geophys. Res.*, this issue.

Hollingsworth, A., D.B. Shaw, P. Lonnberg, L. Illari, K. Arpe, and A.J. Simmons, Monitoring of observations and analysis quality by a data assimilation system, *Mon. Wea. Rev.*, 114, 861-879, 1986.

Johnson, C.J., J. Henshaw, and G. McInnes, Impact of aircraft and surface emissions of nitrogen oxides on tropospheric ozone and global warming, *Nature,* 355, 69-71, 1992

Kain, J.S., and J.M. Fritsch, *Convective Parameterization for Mesoscale Models: The Kain-Fritsch Scheme. The Representation of Cumulus Convection in Numerical Models*, edited by K.A. Emanuel and D.J. Raymond, 246 pp., Amer. Meteorol. Soc., Boston, Mass., 1993.

Kasibhatla, P.S., NO_y from sub-sonic aircraft emissions: A global three-dimensional model study, *Geophys. Res. Lett.*, *20*, 1707-1710, 1993.

Krishnamurti, T.N., H.E. Fuelberg, M.C. Sinhia, D. Oosterhof, E.L. Bensman, and V.B. Kumar, The meteorological environment of the tropospheric ozone maximum over the tropical South Atlantic Ocean, *J. Geophys. Res.*, *98*, 10,621-10,641, 1993.

Pickering, K.E., A.M. Thompson, Y. Wang, W-K. Tao, D.P. McNamara, V.W.J.H. Kirchhoff, B.G. Heikes, G.W. Sachse, J.D. Bradshaw, G.L. Gregory, and D.R. Blake, Convective transport of biomass burning emissions over Brazil during TRACE A, *J. Geophys. Res.*, *101*, 23993-24012, 1996.

Reisner, J., R.T. Bruintjes, and R.J. Rasmussen, Preliminary comparisons between MM5 NCAR/Penn State model generated icing forecasts and observations, *Fifth Intl. Conf. on Aviation Weather Systems, Preprint*, 65-69, 1993.

Schulte, P., and H. Schlager, In-flight measurements of cruise altitude nitric oxide emission indices of commercial jet aircraft, *Geophys. Res. Lett.*, 23, 165-168, 1996.

Schlager, H., P. Konopka, P. Schulte, U. Schumann, H. Ziereis, F. Arnold, M. Klemm, D.E. Hagen, P.D. Whitefield, and J. Ovarlez, In situ observations of air traffic emission signatures in the North Atlantic flight corridor, *J. Geophys. Res.*, 102, 10739-10750, 1997/

Schumann, U., J. Ström, R. Busen, R. Baumann, K. Gierens, M. Krautstrunk, F.S. Schröder, and J. Stingl, In situ observations of particles in jet aircraft exhausts and contails for different sulfur containing fuel, *J. Geophys. Res.*, *101*, 6853-6869, 1996.

Singh. H.B., A.M. Thompson, and H. Schlager, The 1997 SONEX aircraft campaign: Overview and accomplishments, *Geophys. Res. Lett.*, 1999.

Stauffer, D.R., and N.L. Seaman, Use of four-dimensional data assimilation in a limited-area mesoscale model. Part I: Experiments with synoptic-scale data, *Mon. Wea. Rev.*, *118*, 1250-1277, 1990.

Stauffer, D.R., N.L. Seaman, and F.S. Binkowski, Use of four-dimensional data assimilation in a limited-area mesoscale model. Part II: Effects of data assimilation within the planetary boundary layer, *Mon. Wea. Rev.*, *119*, 734-754, 1991.

Stauffer, D.R., and N.L. Seaman, Multiscale four-dimensional data assimilation, *J. Appl. Meteor.*, *33*, 416-434, 1994.

Tyson, P.D., M. Garstang, and R. Swap, Large-scale recirculation of air over southern Africa, *J. Appl. Meteorol.*, 35, 2218-2235, 1996

Wang, Y., W.-K. Tao, K.E. Pickering, A.M. Thompson, J.S. Kain, R.F. Adler, J. Simpson, P.R. Keehn, and G.S. Lai, Mesoscale model simulations of TRACE A and preliminary regional experiment for storm-scale operational and research meteorology convective systems and associated tracer transport, *J. Geophys. Res.*, 101, 24013-24027, 1996.

Warner, T.T., R.A. Peterson, and R.E. Treadon, A tutorial on lateral boundary conditions as a basic and potentially serious limitation to regional numerical weather prediction, *Bull. Amer. Meteorol. Soc.*, *78*, 1997.

Whitefield, P.D., D.E. Hagen, and H. Schlager, Particulate emissions in the exhaust plume from commercial aircraft under cruise conditions, *J. Geophys. Res.*, 101, 19551-19557, 1996.

Zhang, D.-L., and R.A. Anthes, A high-resolution model of the planetary boundary layer sensitivity tests and comparisons with SESAME-79 data, *J. Appl. Meteorol., 21*, 1594-1609, 1982.

Table 1. Number of Aircraft Traversing the NAFC on October 24-25, 1997.

	October 24	October 25
Eastbound	380	391
Westbound	466	458

Table 2. MM5 Model Specifications.

	Model Domain	
	90 km	30 km
Horizontal Grid Points	120x180	157x181
Vertical Sigma Levels	31	31
Cumulus Scheme	Anthes-Kuo	Kain-Fritsch
PBL Scheme	Blackadar	Blackadar
Explicit Moisture Scheme	Reisner Mixed Phase	Reisner Mixed Phase
Model Integration	40 Hours	40 Hours
FDDA	Yes	Yes

Table 3. Trajectory Simulation Periods

Sampling Region	Arrival Time	Beginning Time	Duration
AC1	0900 UTC Oct 25	0600 UTC Oct 24	27 Hours
STRAT	1100 UTC Oct 25	0600 UTC Oct 24	29 Hours
POL-A	1300 UTC Oct 25	0600 UTC Oct 24	31 Hours
POL-B	1400 UTC Oct 25	0600 UTC Oct 24	32 Hours
AC2	1500 UTC Oct 25	0600 UTC Oct 24	33 Hours

Table 4. Results of the aircraft flagging scheme on October 24-25, 1997.

	Number of Aircraft Encountered					
	AC1	STRAT	POL-A	POL-B	AC2	
0600-0700 UTC 24th	2	1	0	0	3	Eastbound
0700-0800 UTC 24th	3	3	0	0	5	Corridor Period
0800-0900 UTC 24th	2	0	0	0	5	
0900-1000 UTC 24th	0	2	0	0	3	
1000-1100 UTC 24th	2	0	0	0	4	
1100-1200 UTC 24th	4	0	0	1	15	
1200-1300 UTC 24th	7	1	0	0	21	
1300-1400 UTC 24th	3	3	0	0	12	
1400-1500 UTC 24th	0	1	0	1	13	Westbound
1500-1600 UTC 24th	1	1	0	0	6	Corridor Period
1600-1700 UTC 24th	1	0	0	0	5	
1700-1800 UTC 24th	2	0	0	0	4	
1800-1900 UTC 24th	0	1	0	0	2	
1900-2000 UTC 24th	1	0	0	0	0	
2000-2100 UTC 24th	1	0	0	0	0	
2100-2200 UTC 24th	2	0	0	0	1	
2200-2300 UTC 24th	2	0	0	0	1	
2300-0000 UTC 25th	1	0	0	0	1	
0000-0100 UTC 25th	1	0	0	0	0	

Time						
0100-0200 UTC 25th	0	0	0	0	0	
0200-0300 UTC 25th	1	1	0	0	1	
0300-0400 UTC 25th	7	1	0	0	9	
0400-0500 UTC 25th	9	0	0	0	3	Eastbound Corridor Period
0500-0600 UTC 25th	10	1	0	0	6	
0600-0700 UTC 25th	2	0	0	0	6	
0700-0800 UTC 25th	7	0	0	0	5	
0800-0900 UTC 25th	6	0	0	0	2	
0900-1000 UTC 25th	0	0	0	0	3	
1000-1100 UTC 25th	0	0	0	1	6	
1100-1200 UTC 25th	0	0	0	0	3	
1200-1300 UTC 25th	0	0	0	0	0	
1300-1400 UTC 25th	0	0	0	0	1	Westbound Corridor Period
1400-1500 UTC 25th	0	0	0	0	0	
TOTALS	77	16	0	3	146	

Plate Captions

Plate 1.   Altitude profile of Flight 8 as a function of latitude. Chemical signatures are indicated by the four colored segments.
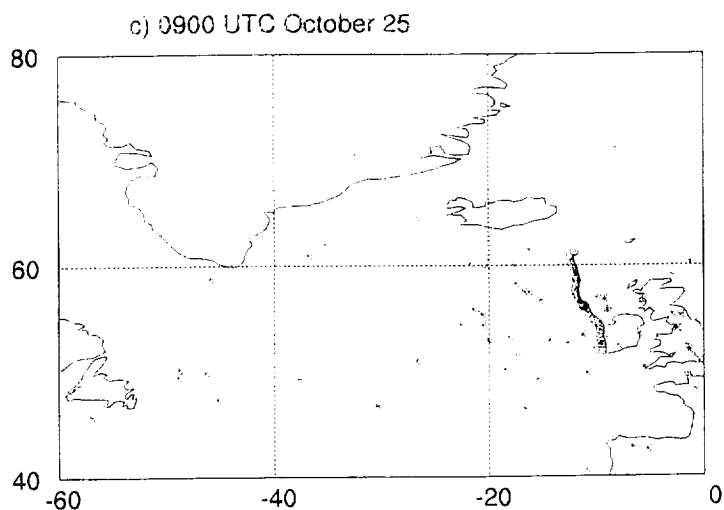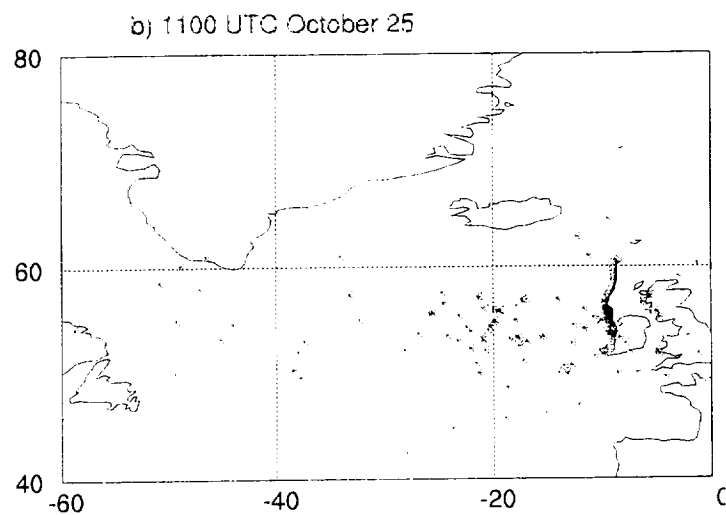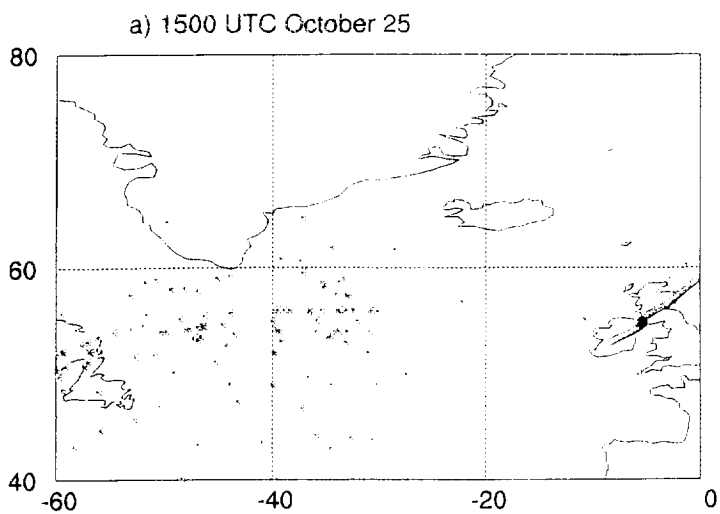
Plate 2.   Plots of aircraft locations and trajectories that arrive in chemical region AC2. The various panels correspond to times on October 24-25, 1997. Trajectory locations are denoted by circles, while aircraft locations are denoted by asterisks. Pink symbols indicate that no trajectory/aircraft encounter occurred based on the flagging scheme described in the text. Blue symbols indicate that a trajectory/aircraft encounter did occur.
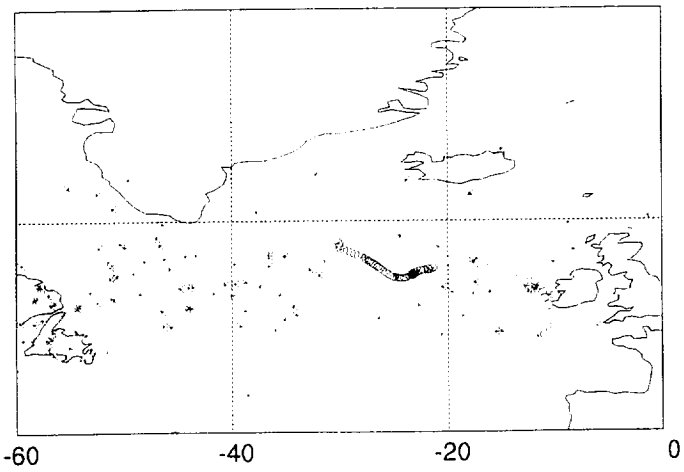
Figure Captions

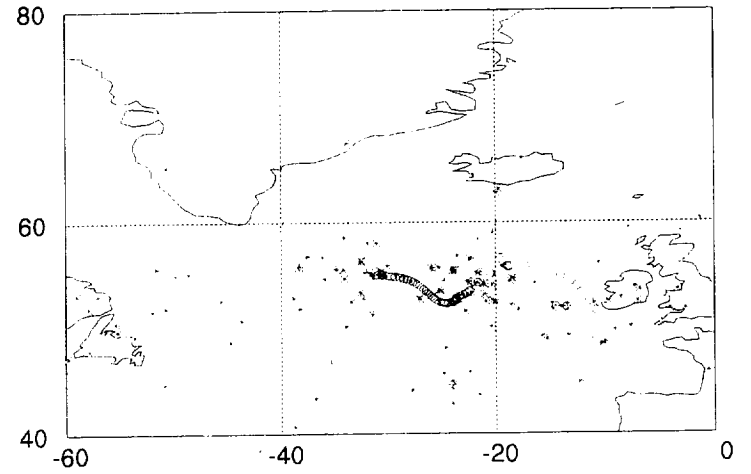Figure 1.   Flight track of the DC-8 on October 25, 1997.

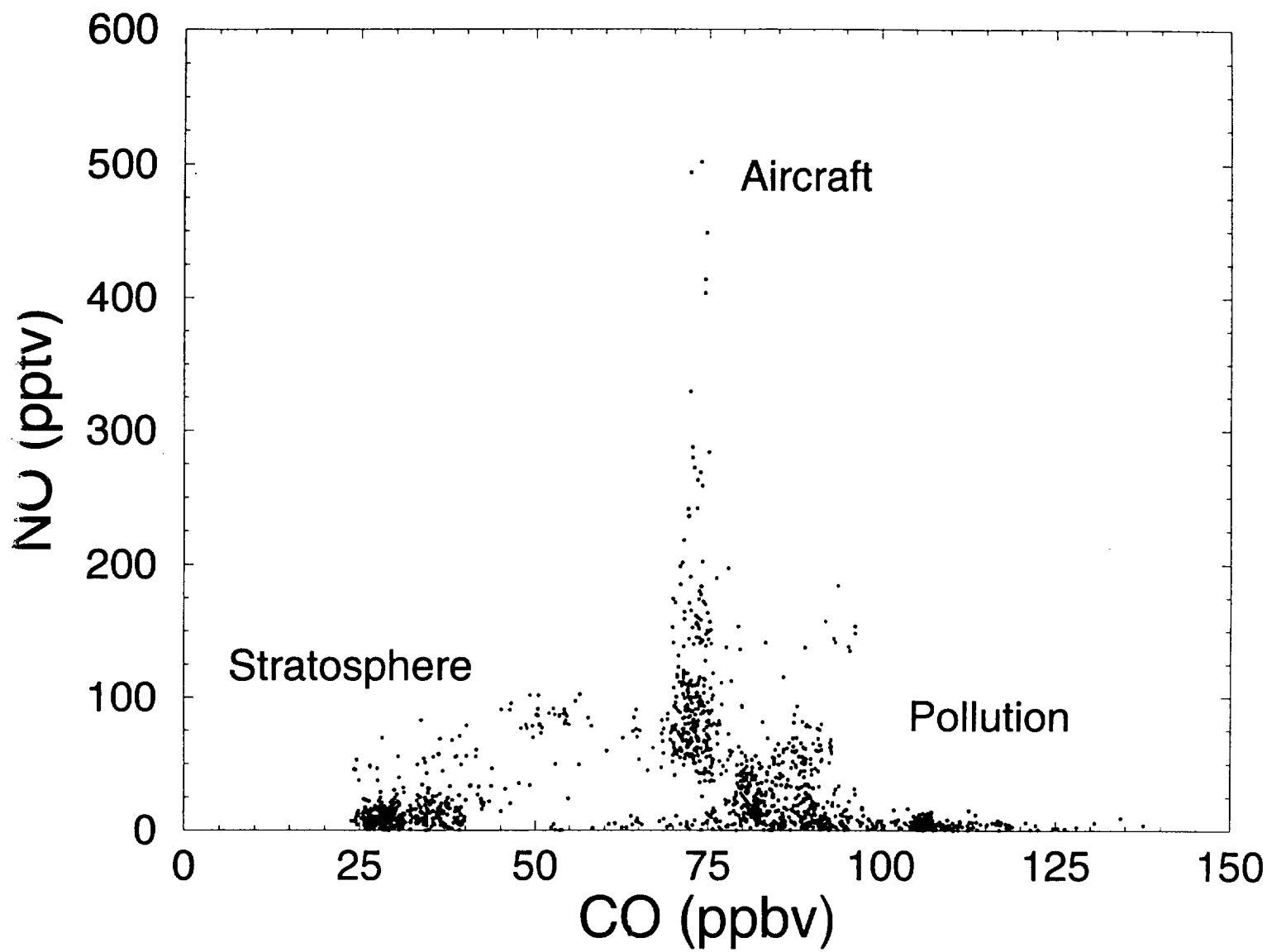Figure 2.   Scatter plot of CO vs NO during SONEX Flight 8. Three chemical signatures are indicated.

Figure 3.   Time series of chemical species and DC-8 altitude along Flight 8. Plots of NO (pptv), NOy (pptv), NO/NOy, O_3 (ppbv), CO (ppbv), and unheated fine aerosols (CN, cm^{-3}) are given in the top six panels. The bottom panel indicates the altitude of the DC-8. Chemical signature regions are labeled on the top panel.
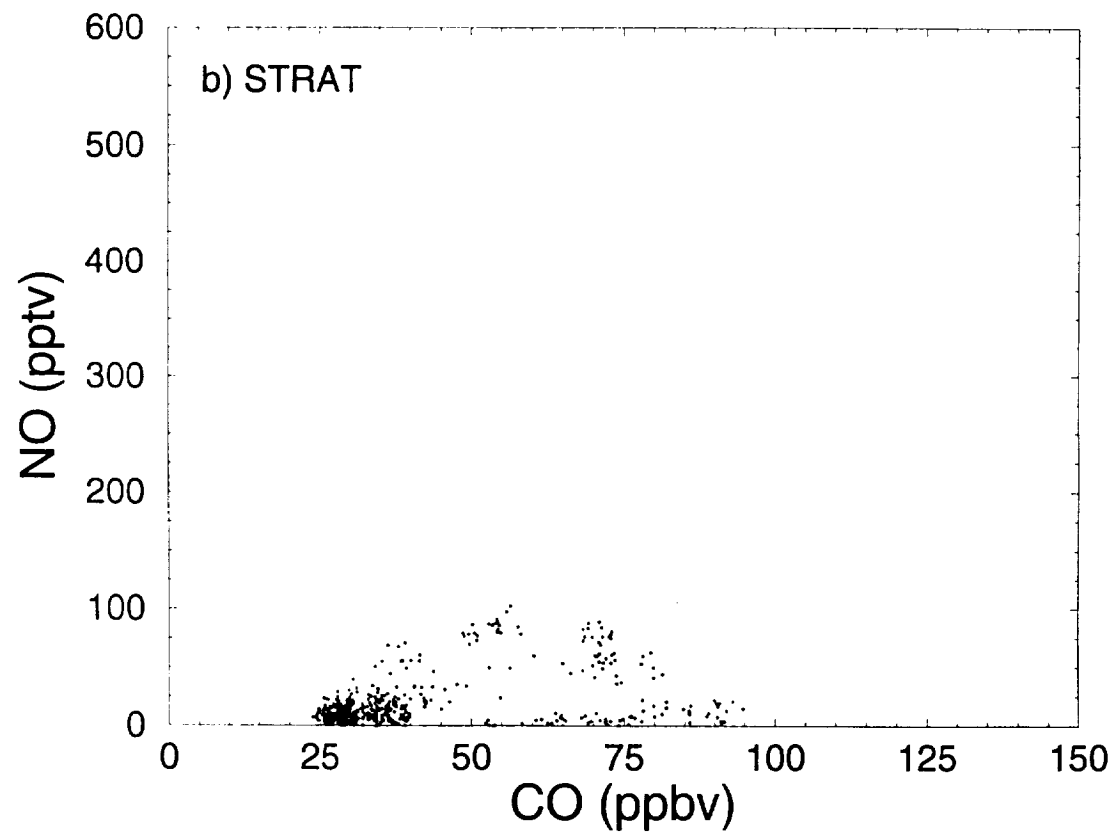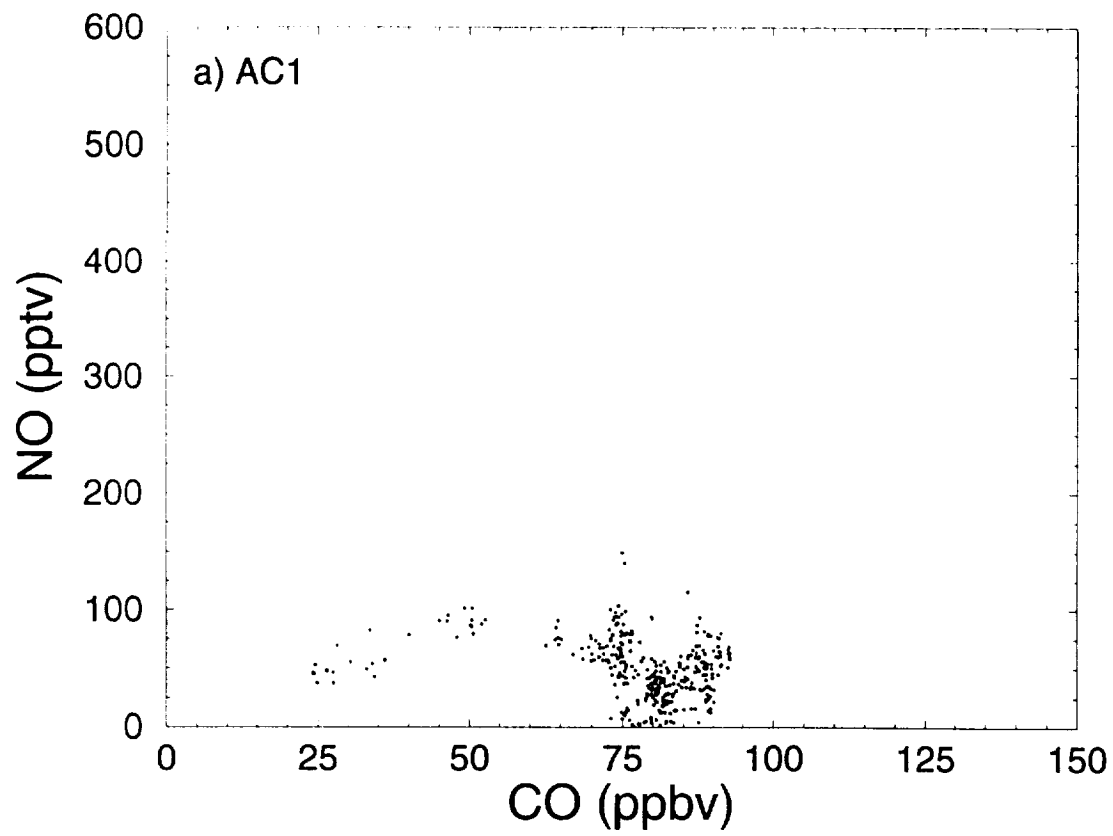
Figure 4.   Scatter plots of CO vs NO for the four chemical signature regions of

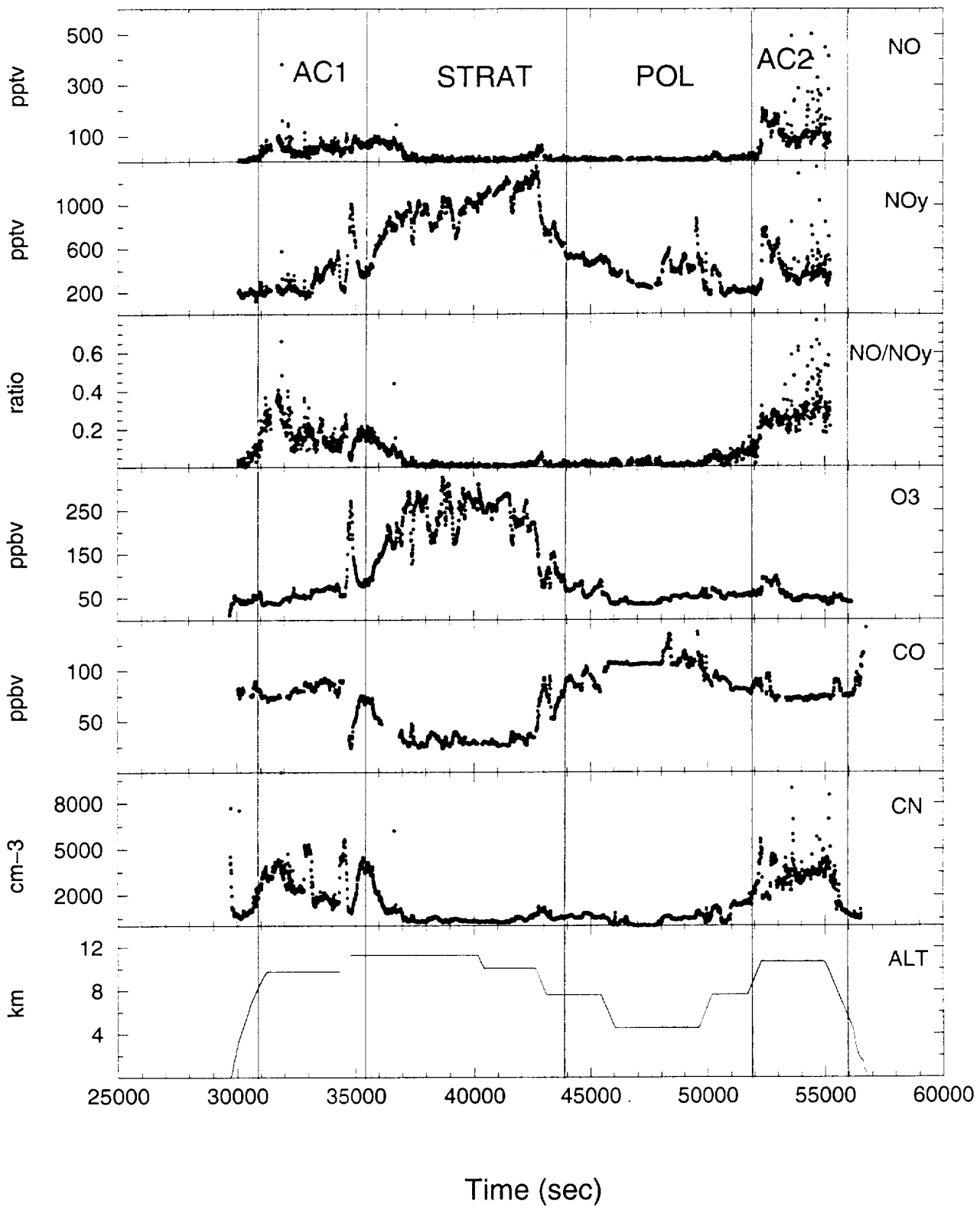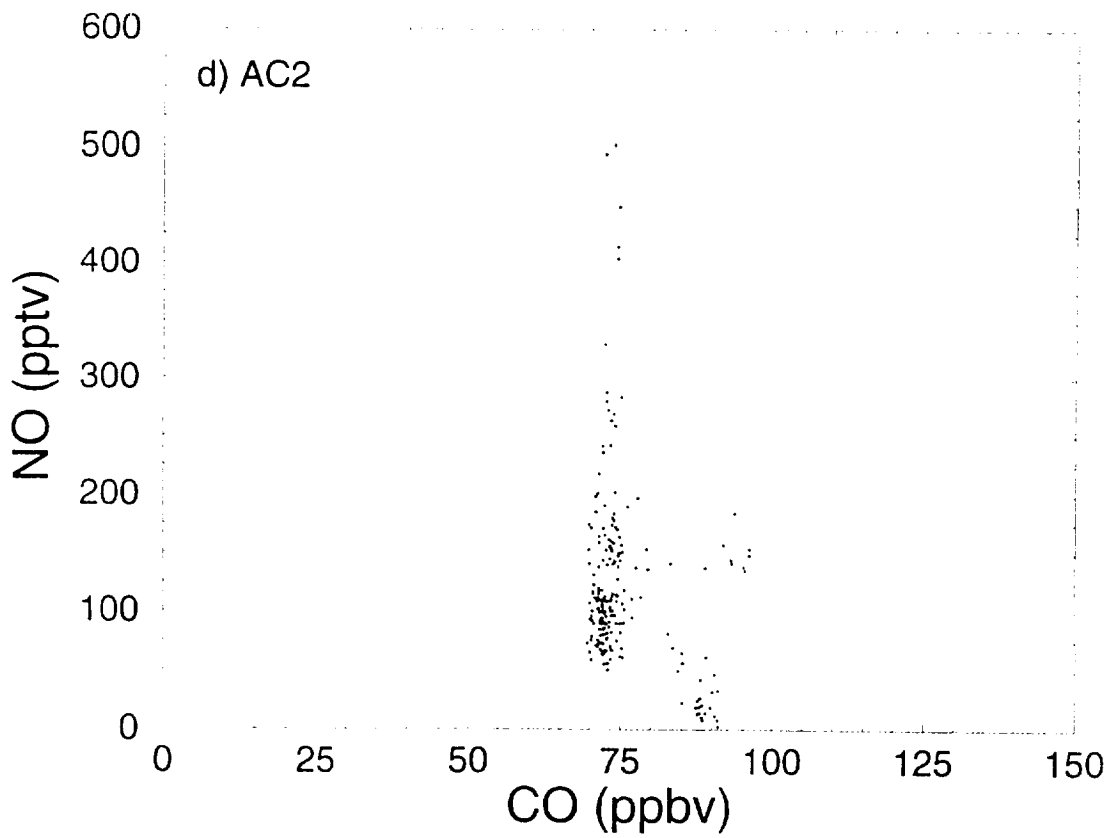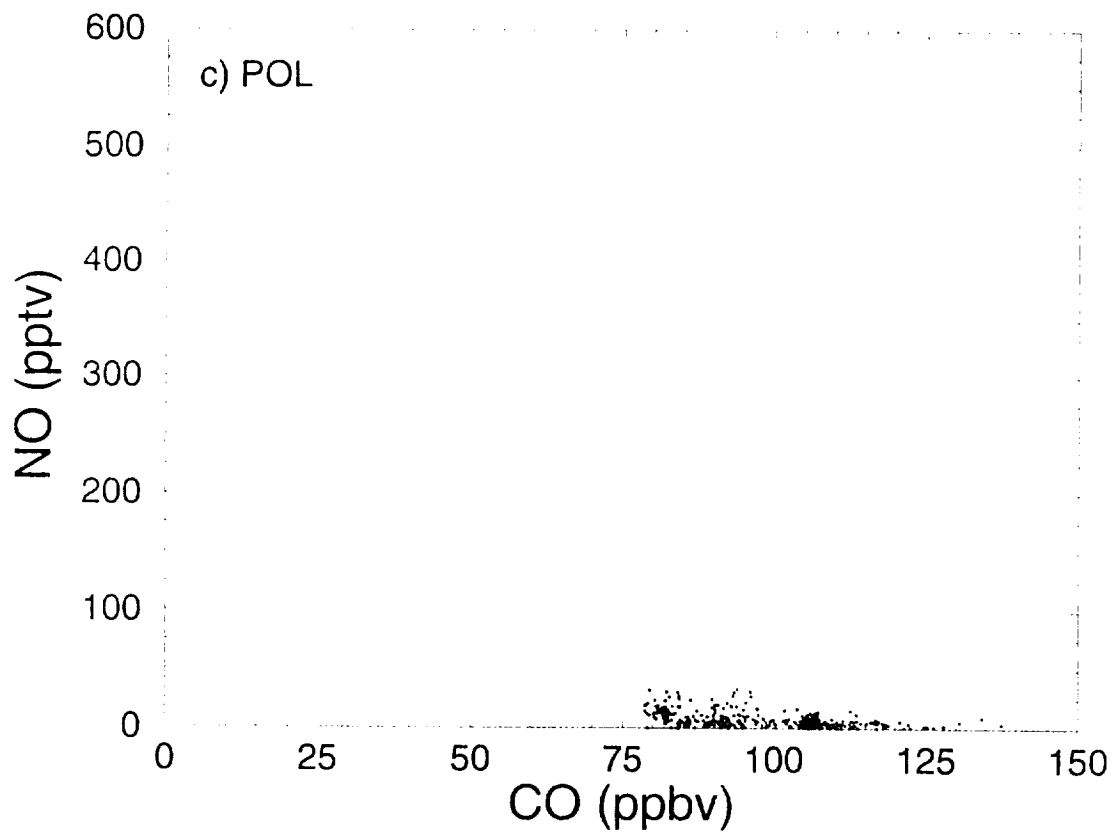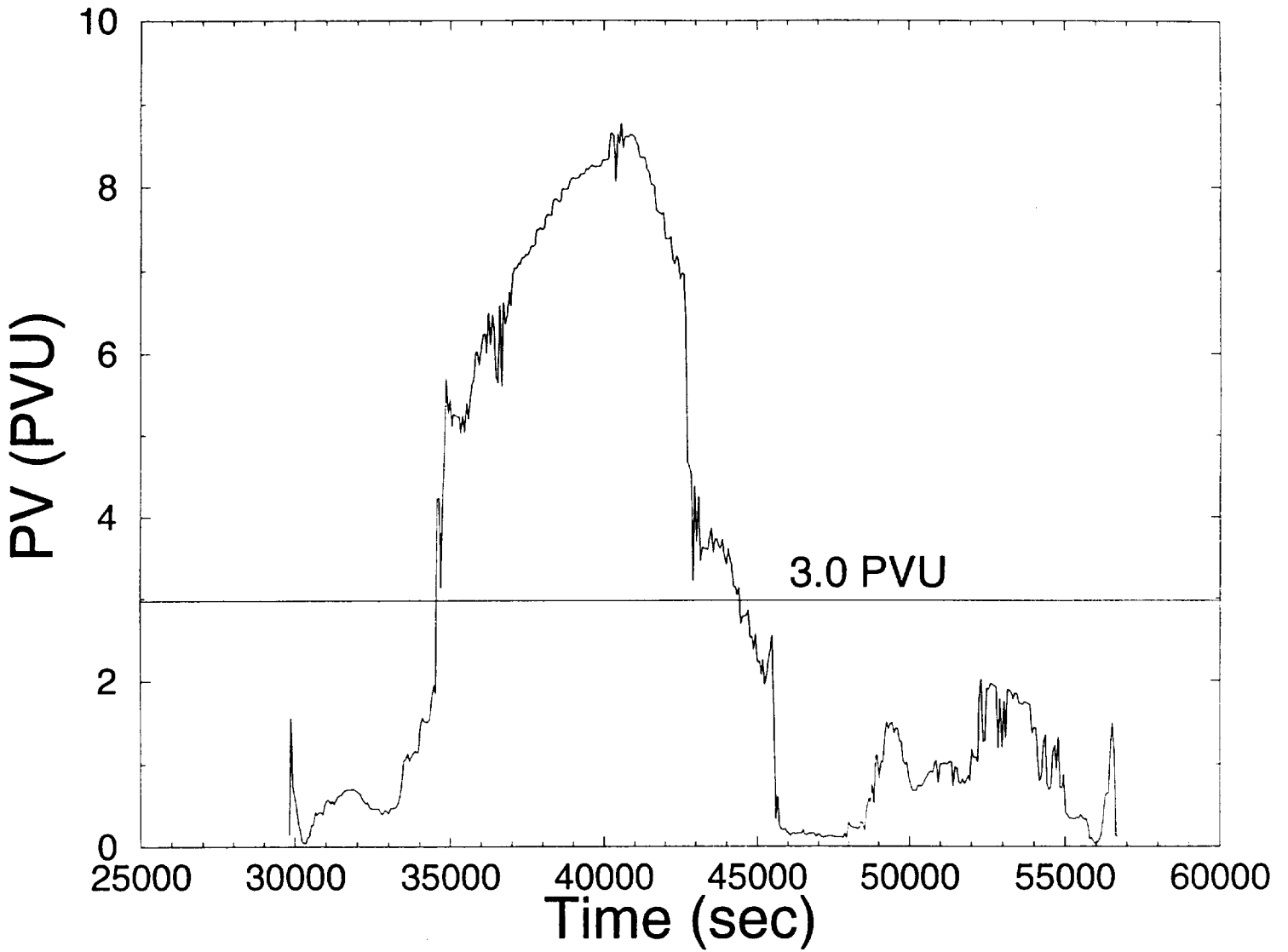Flight 8, a) aircraft 1, b) stratospheric, c) pollution, and d) aircraft 2.

Figure 5.   Time series of flight level potential vorticity (PVU) along Flight 8, where

1 PVU = 1×10^{-5} K mb^{-1} s^{-1}. The 3 PVU stratospheric threshold is

indicated. Values were derived from ECMWF global analyses.

Figure 6.   Flight tracks within the NAFC on October 24, 1997, a) eastbound flights

between 0100-0800 UTC, and b) westbound flights between 1130-1800

UTC. All flights cross 30°W at latitudes between 40°-60°N. Cruising

altitudes are shown in Figure 7.

Figure 7.   Cruising altitudes of the flights within the NAFC that are shown in Figure

6, a) eastbound flights, and b) westbound flights.

Figure 8.   Domains for the MM5 simulations. The outer perimeter indicates the

boundary of the 90 km domain. The inner box represents the area of the

30 km domain. The track of Flight 8 is indicated within the 30 km

domain.

Figure 9.   a) ECMWF analysis of geopotential height (meters) and isotachs (m s^{-1}) at

250 hPa on 1200 UTC October 25.

b) As in a), but the 36 hour MM5-derived analysis.

c) ECMWF analysis of potential vorticity (PVU) at 250 hPa on 1200 UTC

October 25.

d) As in c), but from the 36 hour MM5 analysis.

Figure 10.   Trajectories arriving at the four chemical signature regions of Flight 8, a)

aircraft 1, b) stratospheric, c) pollution region north of 65°N, d) pollution

region south of 65°N, and e) aircraft 2. Arrival times along the DC-8

33

flight track and other data are given in Table 2. Arrows indicate trajectory locations at 6 hour intervals.

Figure 11.   Trajectory altitude (hPa) as a function of time before arrival in chemical signature regions a) aircraft 1, b) stratospheric, c) pollution region north of 65°N. d) pollution region south of 65°N, and e) aircraft 2.

Figure 12.   (Bottom) Time series of flight level NO (pptv) during Flight 8. Chemical signature regions are indicated, and certain maxima and minima are numbered for discussion in the text.

(Top) Number of aircraft encounters for each trajectory arriving along the flight track. Trajectories were calculated at 1 minute intervals.

SONEX Flight 8
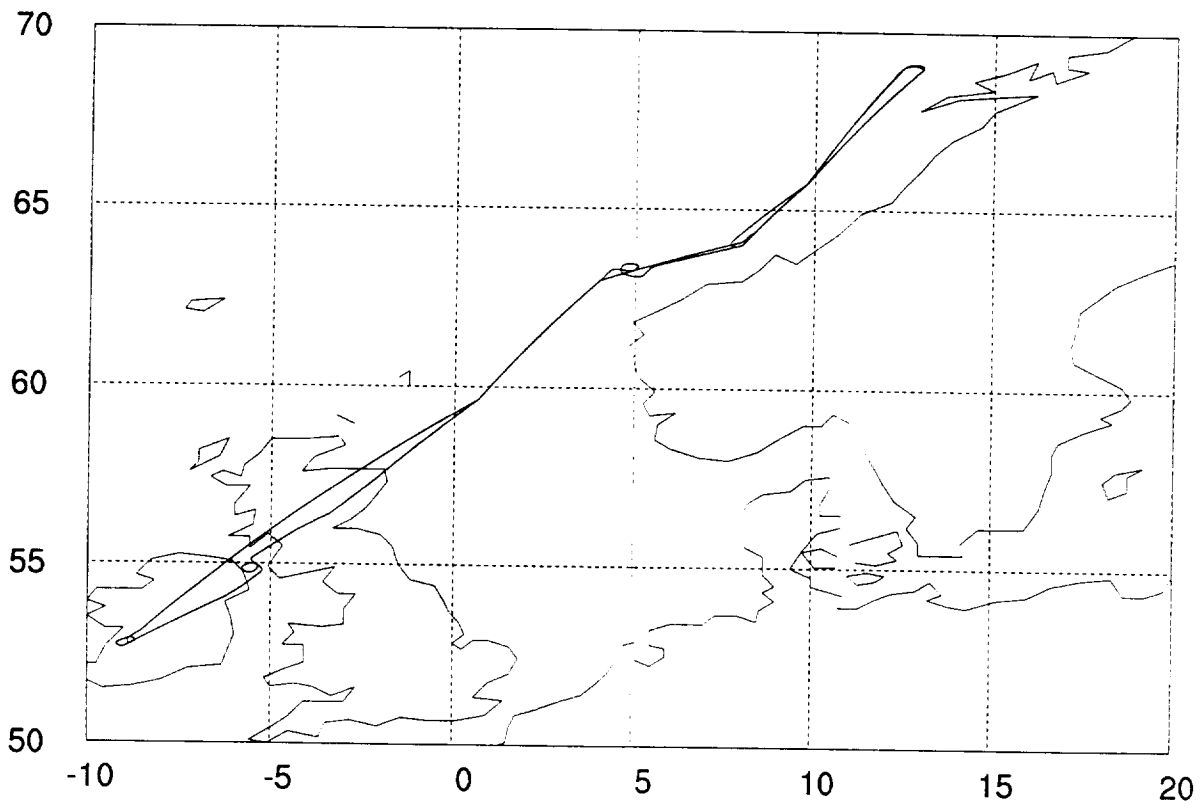
Figure 1.   Flight track of the DC-8 on October 25, 1997.
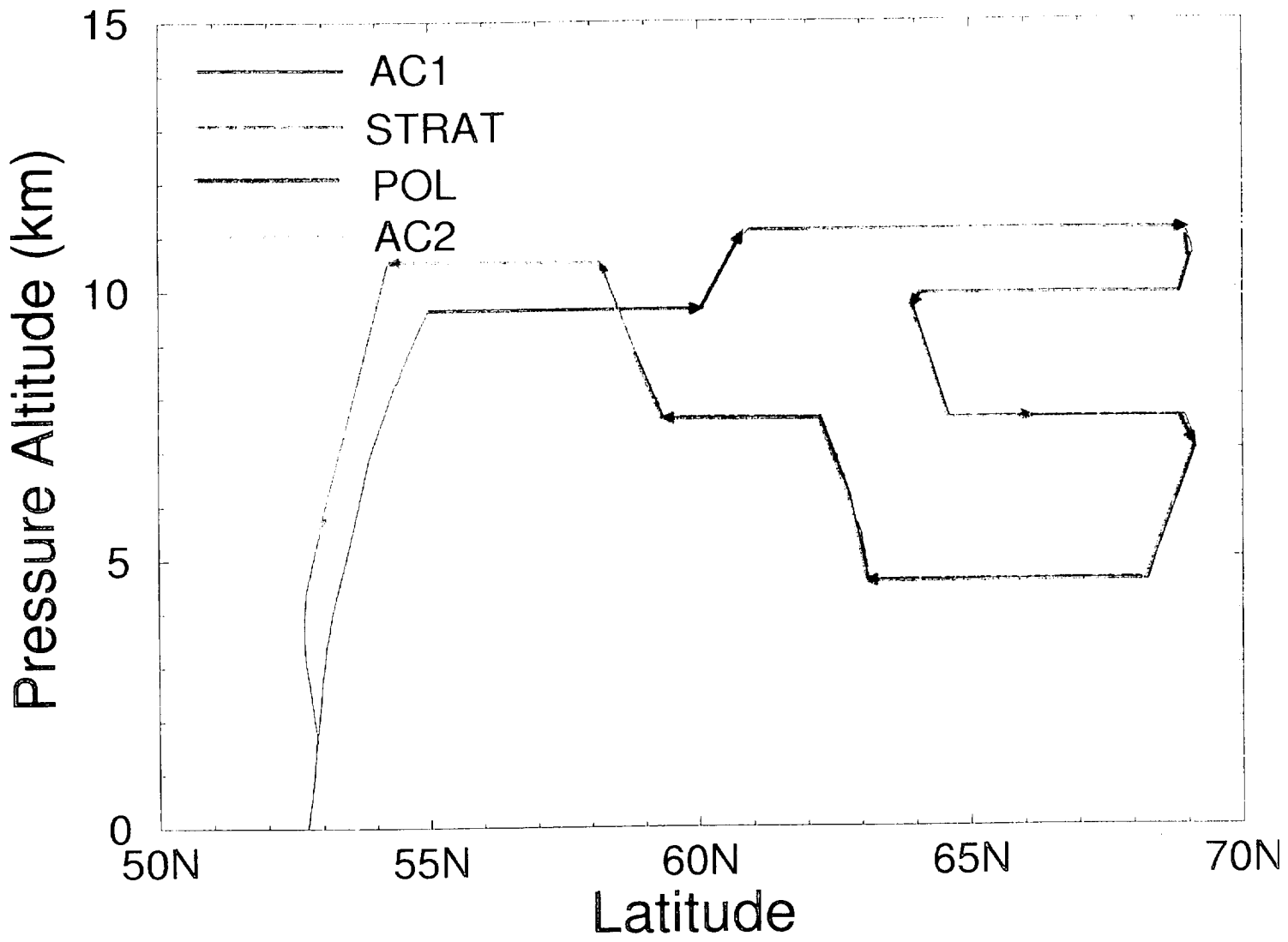
Plate 1.   Altitude profile of Flight 8 as a function of latitude. Chemical signatures are indicated by the four colored segments.

a) 1500 UTC October 25

b) 1100 UTC October 25

c) 0900 UTC October 25

d) 0500 UTC October 25
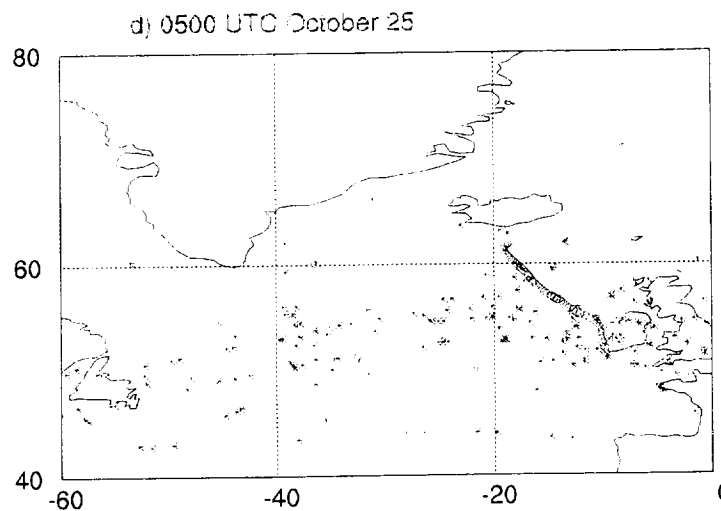
Plate 2.   Plots of aircraft locations and trajectories that arrive in chemical region
             AC2. The various panels correspond to times on October 24-25, 1997.
             Trajectory locations are denoted by circles, while aircraft locations are
             denoted by asterisks. Pink symbols indicate that no trajectory/aircraft
             encounters occurred based on the flagging scheme described in the text.
             Blue symbols indicate that a trajectory/aircraft encounter did occur.

e) 0300 UTC October 25
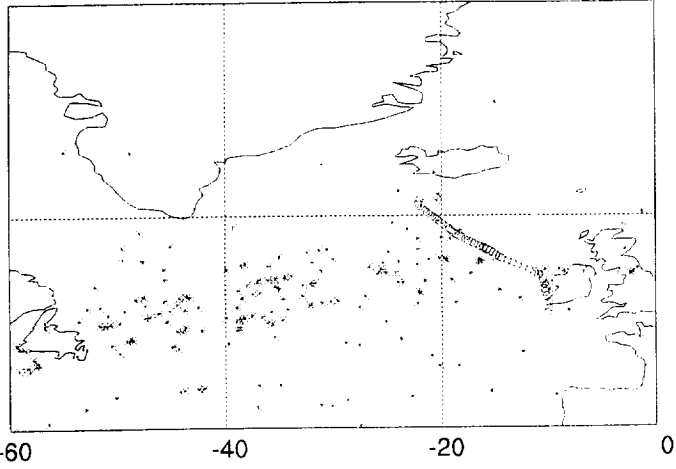
f) 2200 UTC October 24
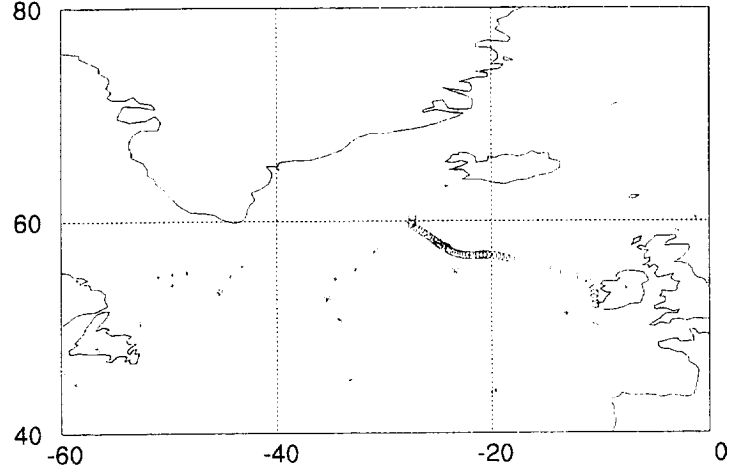
g) 1700 UTC October 24

h) 1200 UTC October 24

Plate 2.   (Continued)

Figure 2.   Scatter plot of CO vs NO during SONEX Flight 8. Three chemical signatures are indicated.

Figure 4.   Scatter plots of CO vs NO for the four chemical signature regions of
              Flight 8, a) aircraft 1, b) stratospheric, c) pollution, and d) aircraft 2.

Figure 3.   Time series of chemical species and DC-8 altitude along Flight 8. Plots of NO (pptv). NOy (pptv), NO/NOy, O_3 (ppbv), CO (ppbv), and unheated fine aerosols (CN, cm^{-3}) are given in the top six panels. The bottom panel indicates the altitude of the DC-8. Chemical signature regions are labeled on the top panel.

Figure 4.   (Continued)

Figure 5.   Time series of flight level potential vorticity (PVU) along Flight 8, where
1 PVU = 1×10^{-5} K mb^{-1} s^{-1}. The 3 PVU stratospheric threshold is
indicated. Values were derived from ECMWF global analyses.

a)
NAFC Eastbound Flights
0100-0800 UTC October 24, 1997
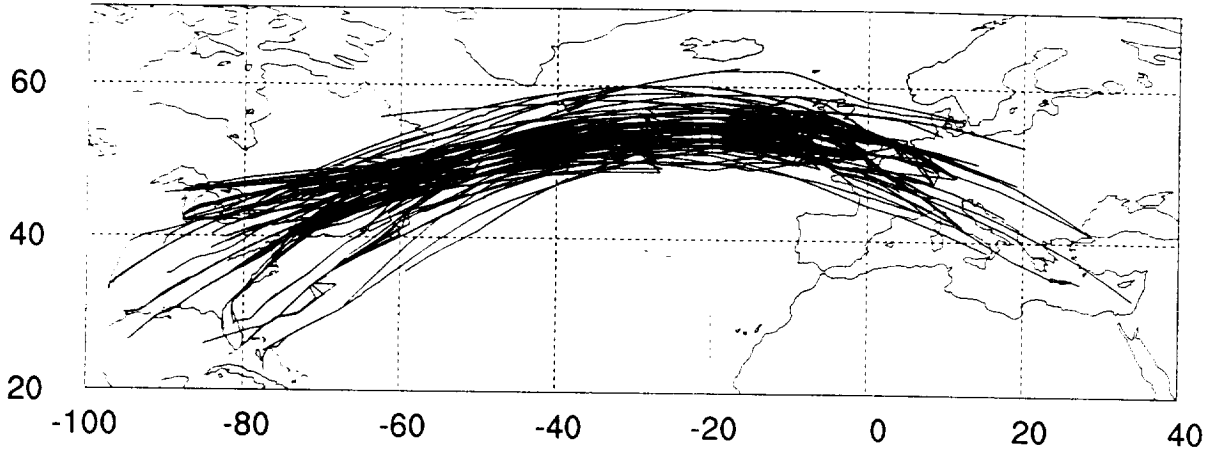
b)
NAFC Westbound Flights
1130-1800 UTC October 24, 1997

Figure 6.   Flight tracks within the NAFC on October 24, 1997, a) eastbound flights between 0100-0800 UTC, and b) westbound flights between 1130-1800 UTC. All flights cross 30°W at latitudes between 40°-60°N. Cruising altitudes are shown in Figure 7.

Figure 7.   Cruising altitudes of the flights within the NAFC that are shown in Figure
6, a) eastbound flights, and b) westbound flights.

Figure 8.   Domains for the MM5 simulations. The outer perimeter indicates the
             boundary of the 90 km domain. The inner box represents the area of the
             30 km domain. The track of Flight 8 is indicated within the 30 km
             domain.

a)

b)

Figure 9.   a) ECMWF analysis of geopotential height (meters) and isotachs (m s⁻¹) at 250 hPa on 1200 UTC October 25.
b) As in a), but the 36 hour MM5-derived analysis.
c) ECMWF analysis of potential vorticity (PVU) at 250 hPa on 1200 UTC October 25.
d) As in c), but from the 36 hour MM5 analysis.

c)

d)

Figure 9.   (Continued)
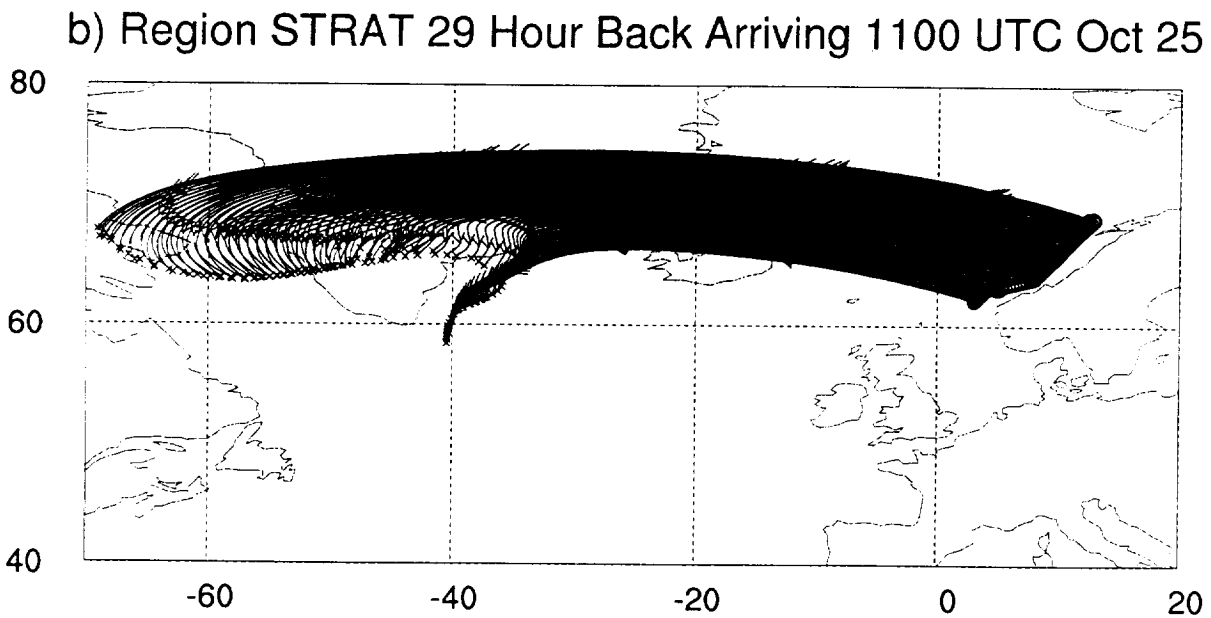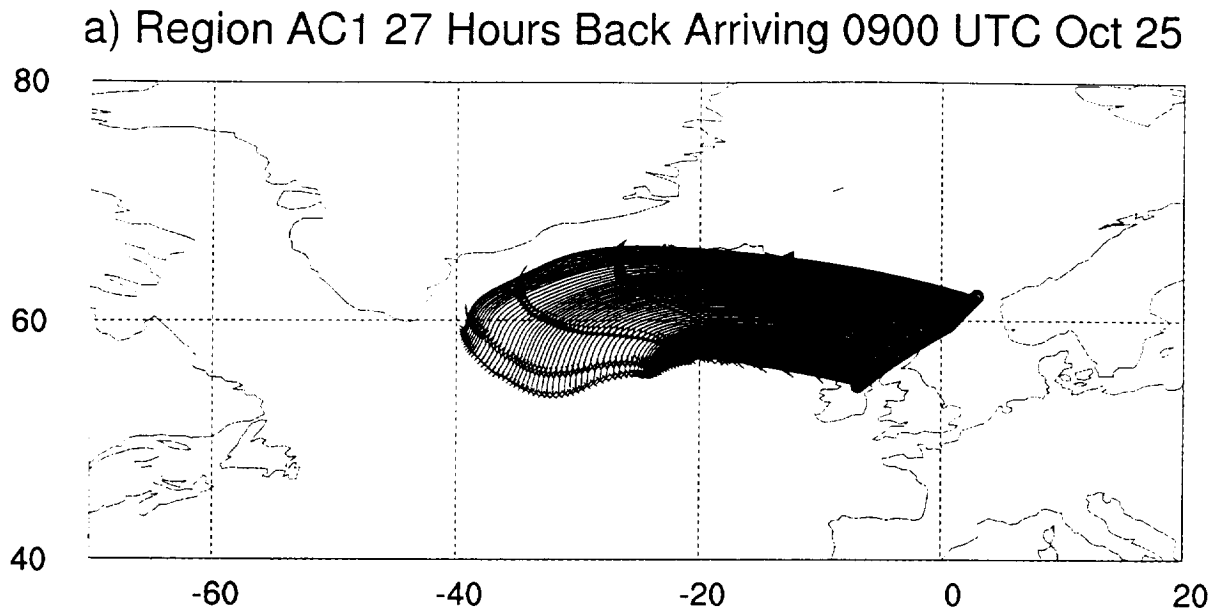
a) Region AC1 27 Hours Back Arriving 0900 UTC Oct 25

b) Region STRAT 29 Hour Back Arriving 1100 UTC Oct 25

Figure 10.   Trajectories arriving at the four chemical signature regions of Flight 8, a)
aircraft 1, b) stratospheric, c) pollution region north of 65°N, d) pollution
region south of 65°N, and e) aircraft 2. Arrival times along the DC-8
flight track and other data are given in Table 2. Arrows indicate trajectory
locations at 6 hour intervals.

c) Region POL-A 31 Hour Back Arriving 1300 UTC Oct 25
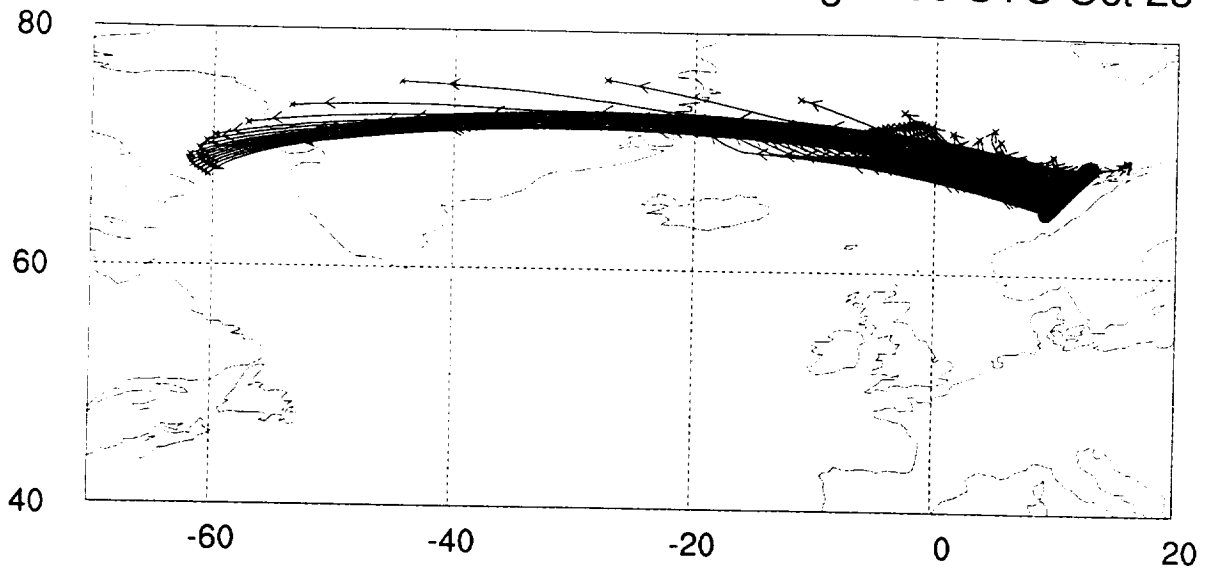
d) Region POL-B 32 Hour Back Arriving 1400 UTC Oct 25
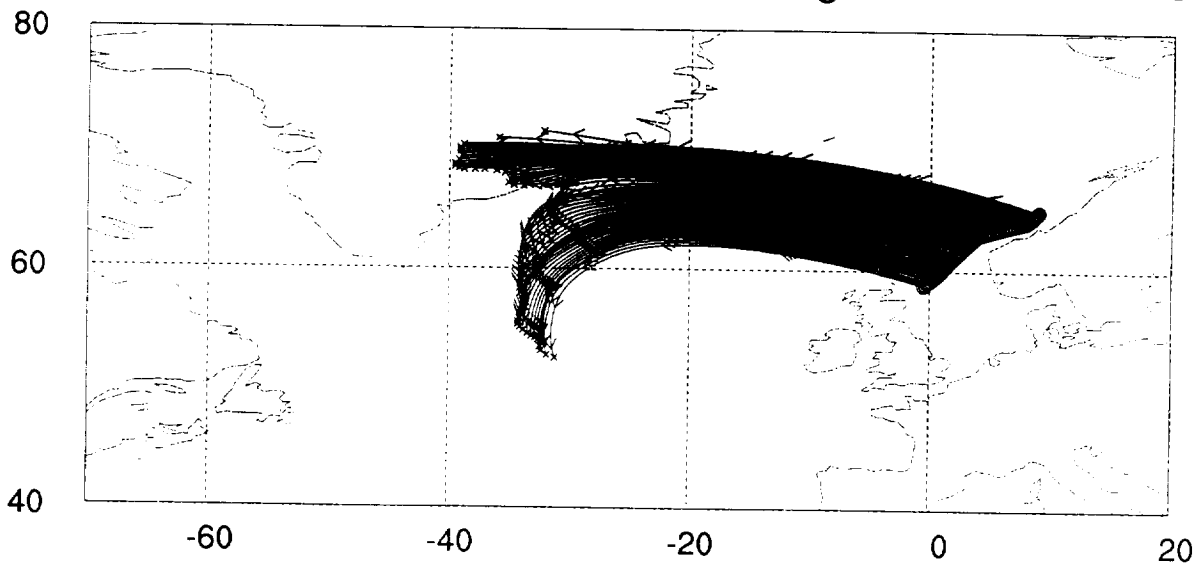
Figure 10.   (Continued)

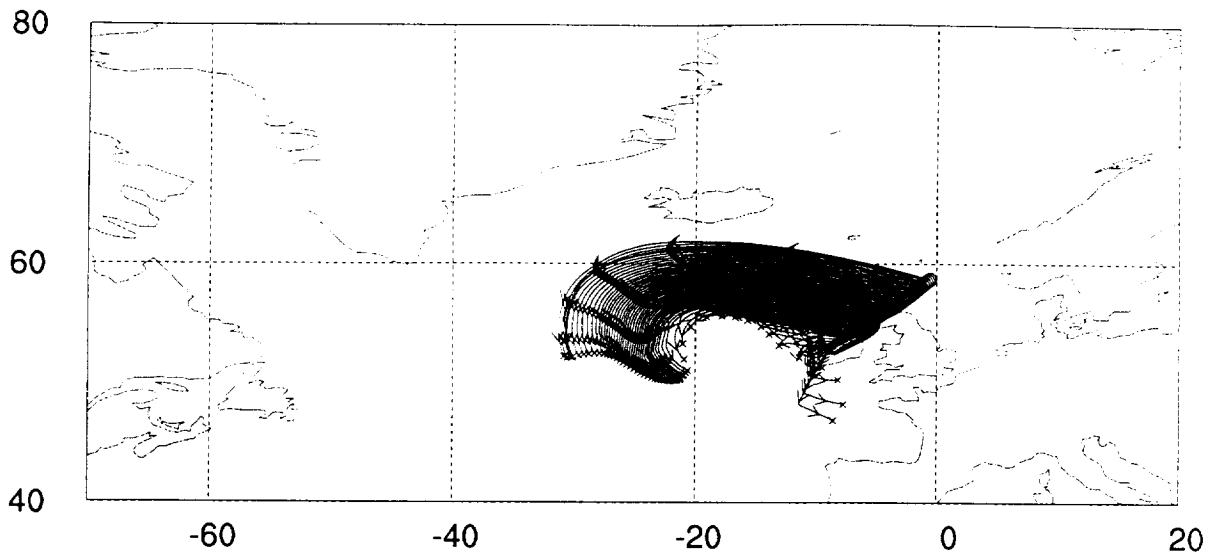## e) Region AC2 33 Hour Back Arriving 1500 UTC Oct 25
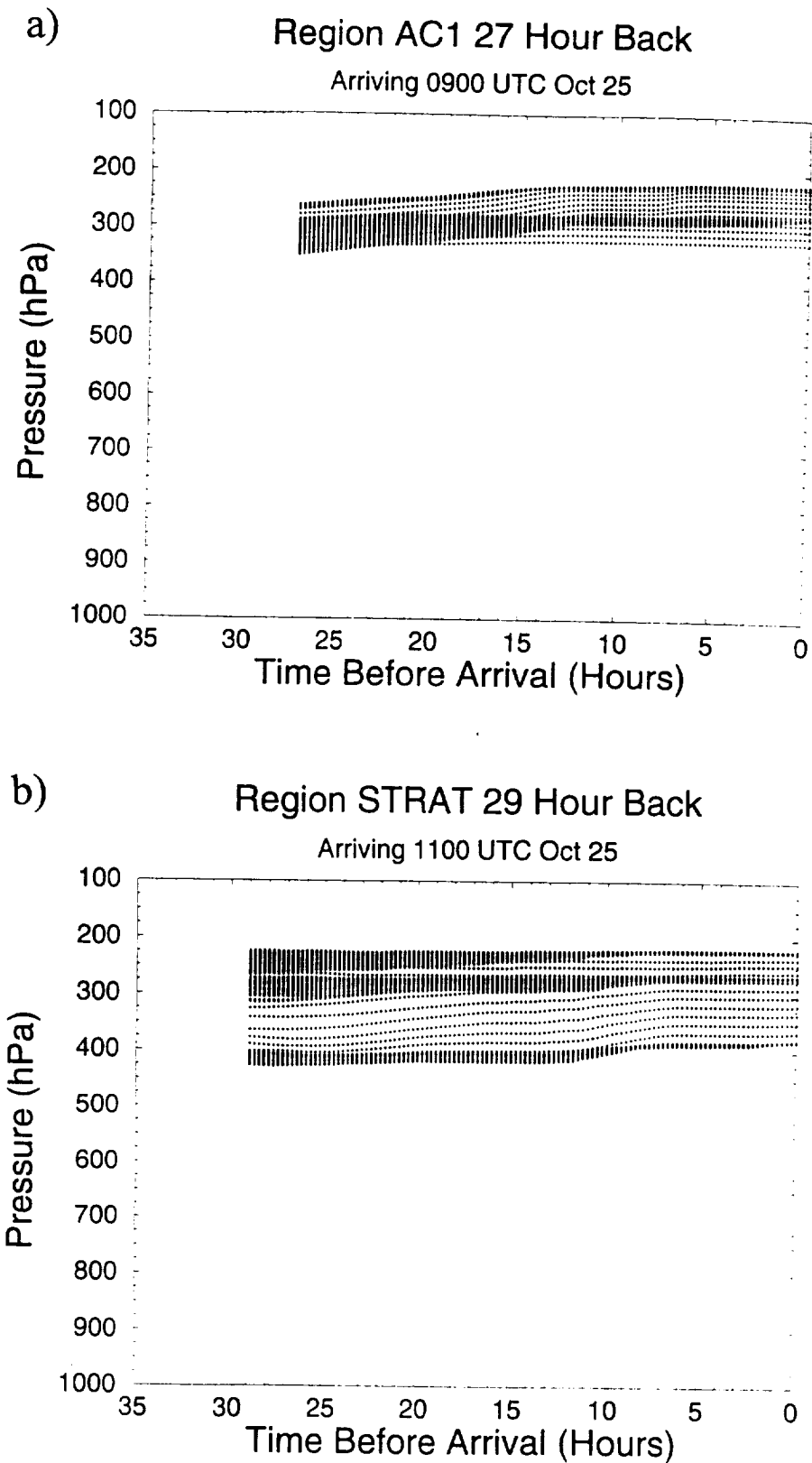

Figure 10.   (Continued)

a) **Region AC1 27 Hour Back**

Arriving 0900 UTC Oct 25

b) **Region STRAT 29 Hour Back**

Arriving 1100 UTC Oct 25

Figure 11.   Trajectory altitude (hPa) as a function of time before arrival in chemical signature regions a) aircraft 1, b) stratospheric, c) pollution region north of 65°N, d) pollution region south of 65°N, and e) aircraft 2.
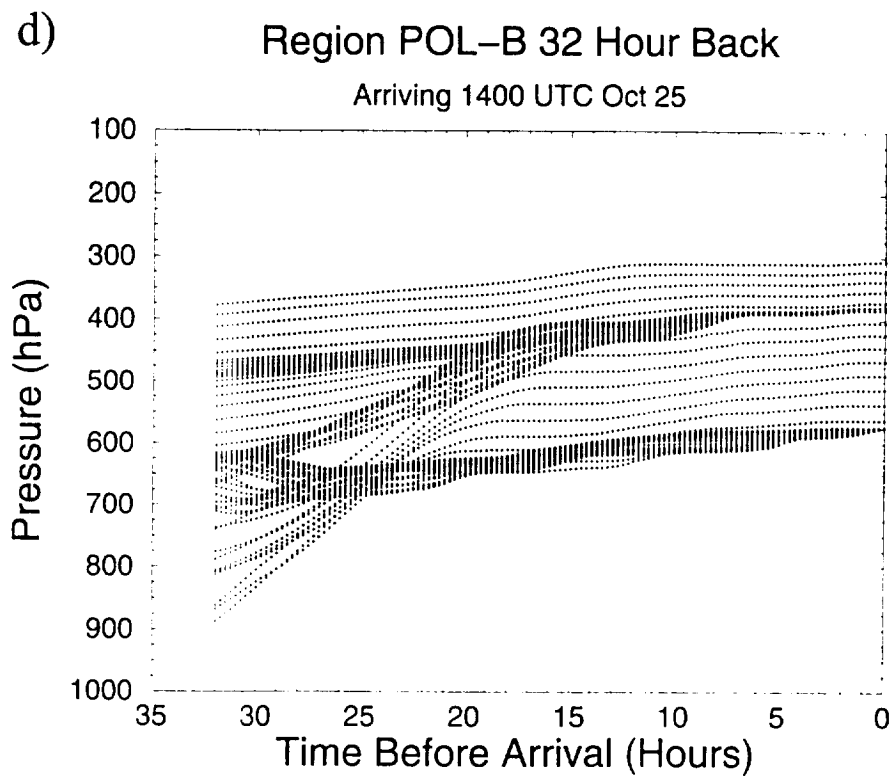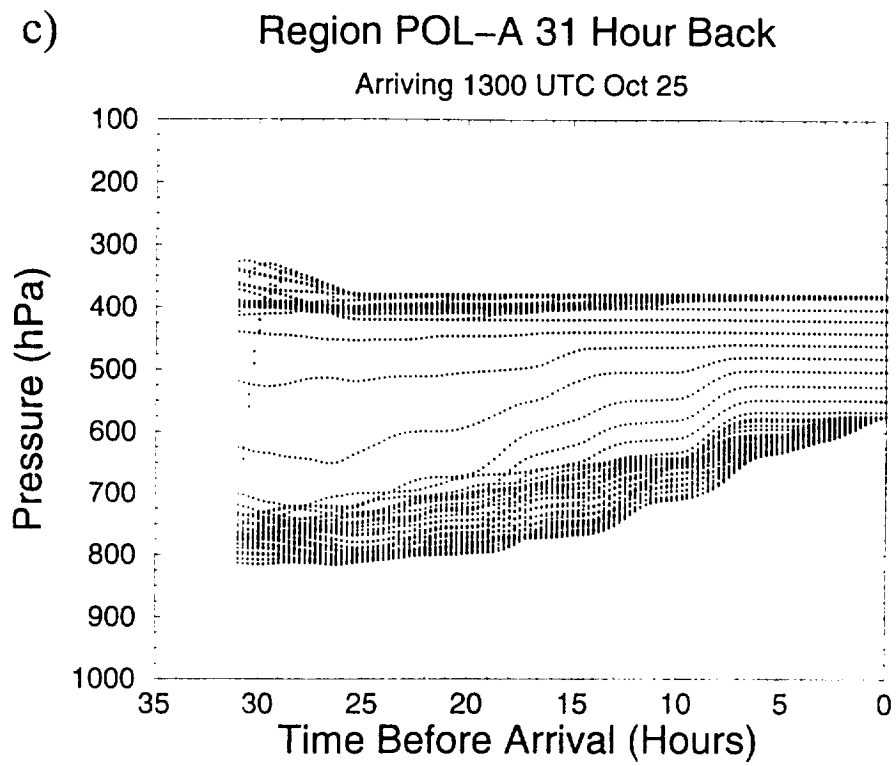
c)

Region POL–A 31 Hour Back

Arriving 1300 UTC Oct 25

d)

Region POL–B 32 Hour Back

Arriving 1400 UTC Oct 25

Figure 11.   (Continued)

e)

Region AC2 33 Hour Back
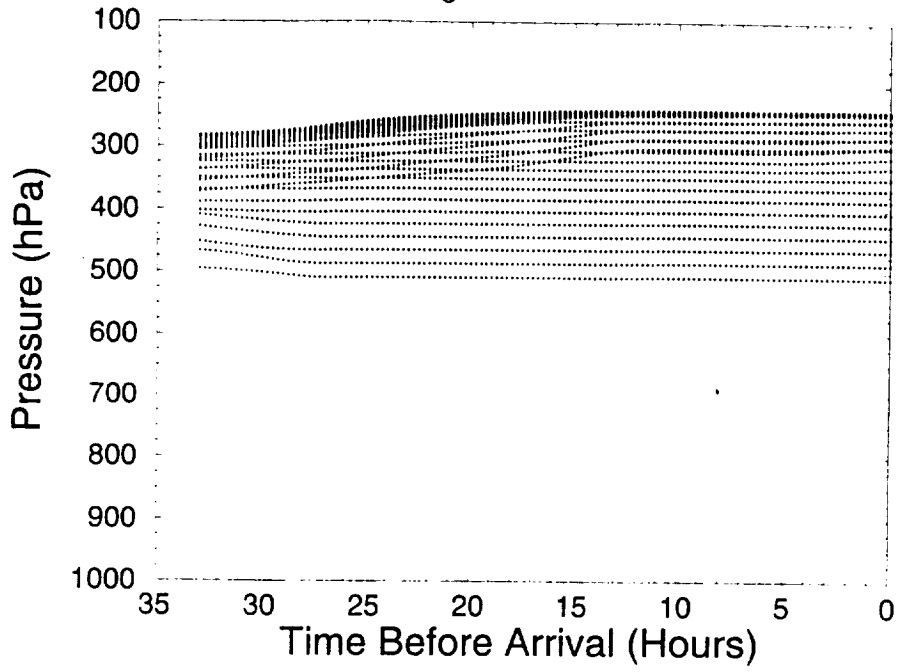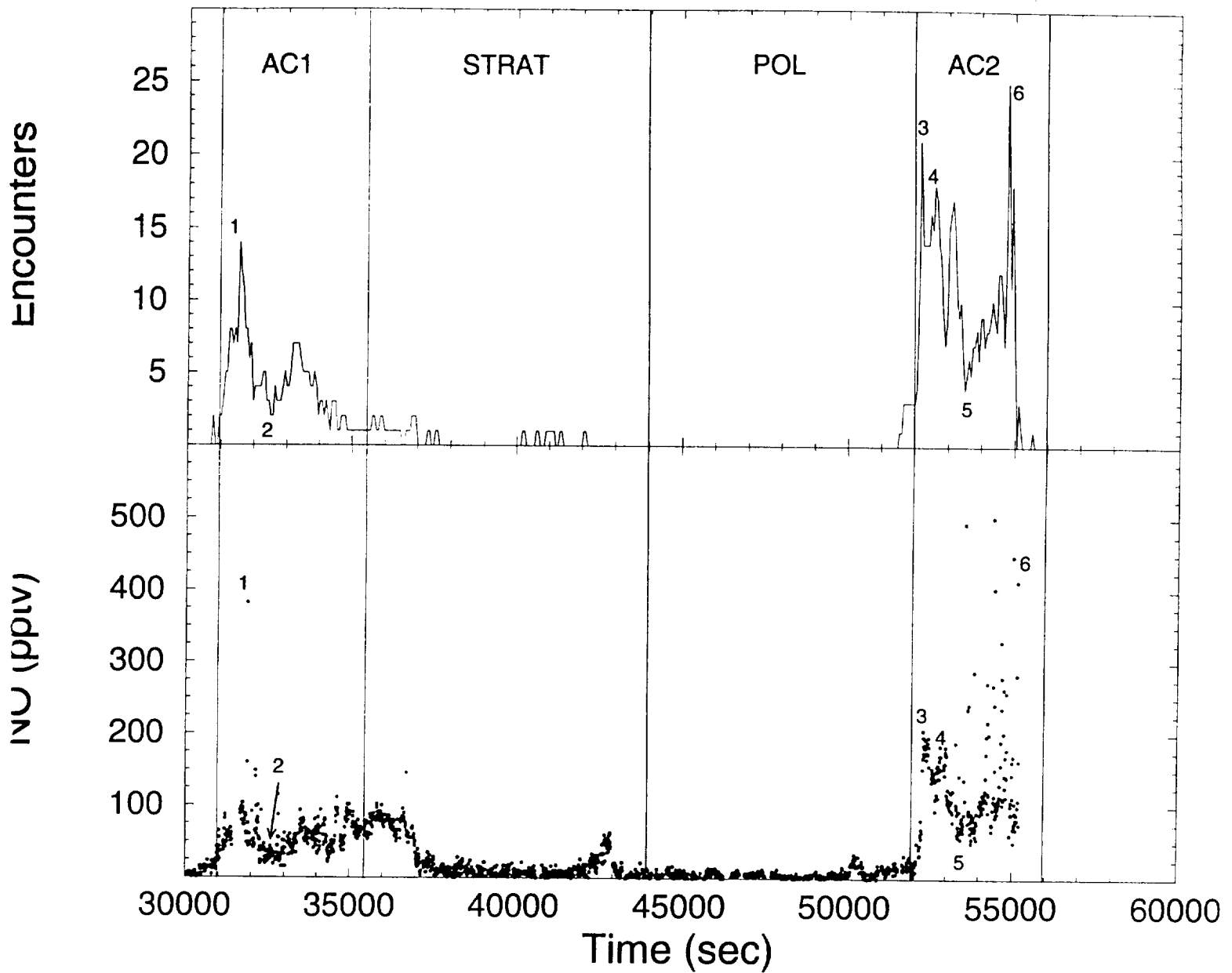### Arriving 1500 UTC Oct 25

Figure 11.   (Continued)

Figure 12.   (Bottom) Time series of flight level NO (pptv) during Flight 8. Chemical
signature regions are indicated, and certain maxima and minima are
numbered for discussion in the text.
(Top) Number of aircraft encounters for each trajectory arriving along the
flight track. Trajectories were calculated at 1 minute intervals.